AD-A244 111

REPORT DOCUMENTATION PAGE

Form Approved
OMB No. 0704-0188

Public reporting ... per response, including the time for reviewing instructions, searching existing data sources, gathering and m... of information. Send comments regarding this burden estimate or any other aspect of this collection of info... Headquarters Services, Directorate for Information Operations and Reports, 1215 Jefferson Davis Highway, S... and Budget, Paperwork Reduction Project (0704-0188), Washington, DC 20503.

1. AGENCY USE ONLY	2. REPORT DATE	3. REPORT TYPE AND DATES COVERED
	November 8, 1991	Final Report 4/1/91 - 9/30/91

4. TITLE AND SUBTITLE
Titanium Carbide-Graphite Composites

5. FUNDING NUMBERS
DAAL03-91-C-0015

6. AUTHOR(S)
Delwyn Cummings

DTIC ELECTE JAN 10 1992 S D D

7. PERFORMING ORGANIZATION NAME(S) AND ADDRESS(ES)
Advanced Technology Materials, Inc
7 Commerce Drive
Danbury, CT 06810

8. PERFORMING ORGANIZATION REPORT NUMBER

92-00753

9. SPONSORING/MONITORING AGENCY NAME(S) AND ADDRESS(ES)
U. S. Army Research Office
P. O. Box 12211
Research Triangle Park, NC 27709-2211

10. SPONSORING/MONITORING AGENCY REPORT NUMBER
ARO 28452.1-MS-SBI

11. SUPPLEMENTARY NOTES
The view, opinions and/or findings contained in this report are those of the author(s) and should not be construed as an official Department of the Army position, policy, or decision, unless so designated by other documentation.

12a. DISTRIBUTION/AVAILABILITY STATEMENT
Approved for public release; distribution unlimited.

12b. DISTRIBUTION CODE

13. ABSTRACT *(Maximum 200 words)*

Pure titanium carbide, titanium carbide with free graphite, titanium carbide/vanadium carbide alloy with free graphite, and titanium carbide with boron and free graphite were tested for friction and wear at 22, 600, and 900°C. Test pins of the four compositions were machined from ingots prepared from melts. The test pins were drawn across hot pressed titanium carbide wear plates with 5 newtons of normal force. The lowest friction coefficient at 22°C was 0.12 obtained with pure titanium carbide. The lowest friction coefficient at 900°C was 0.19 obtained with titanium carbide with boron and free graphite. Titanium carbide based materials offer a great deal of flexibility in terms of possible composite compositions, all of which can be prepared from a melt. Further development in this area would entail selecting a specific application and performing friction and wear tests to optimize behavior under those load, atmosphere, and sliding speed conditions.

14. SUBJECT TERMS
Titanium Carbide, Graphite, Composite, Tribology

15. NUMBER OF PAGES
77

16. PRICE CODE

17. SECURITY CLASSIFICATION OF REPORT	18. SECURITY CLASSIFICATION OF THIS PAGE	19. SECURITY CLASSIFICATION OF ABSTRACT	20. LIMITATION OF ABSTRACT
UNCLASSIFIED	UNCLASSIFIED	UNCLASSIFIED	UL

NSN 7540-01-280-5500

Standard Form 298 (Rev. 2-89)
Prescribed by ANSI Std. Z39-18
298-102

92 1 8 147

GENERAL INSTRUCTIONS FOR COMPLETING SF 298

The Report Documentation Page (RDP) is used in announcing and cataloging reports. It is important that this information be consistent with the rest of the report, particularly the cover and title page. Instructions for filling in each block of the form follow. It is important to *stay within the lines* to meet *optical scanning requirements.*

Block 1. Agency Use Only *(Leave blank)*.

Block 2. Report Date. Full publication date including day, month, and year, if available (e.g. 1 Jan 88). Must cite at least the year.

Block 3. Type of Report and Dates Covered. State whether report is interim, final, etc. If applicable, enter inclusive report dates (e.g. 10 Jun 87 - 30 Jun 88).

Block 4. Title and Subtitle. A title is taken from the part of the report that provides the most meaningful and complete information. When a report is prepared in more than one volume, repeat the primary title, add volume number, and include subtitle for the specific volume. On classified documents enter the title classification in parentheses.

Block 5. Funding Numbers. To include contract and grant numbers; may include program element number(s), project number(s), task number(s), and work unit number(s). Use the following labels:

C	- Contract	PR	- Project
G	- Grant	TA	- Task
PE	- Program Element	WU	- Work Unit Accession No.

Block 6. Author(s). Name(s) of person(s) responsible for writing the report, performing the research, or credited with the content of the report. If editor or compiler, this should follow the name(s).

Block 7. Performing Organization Name(s) and Address(es). Self-explanatory.

Block 8. Performing Organization Report Number. Enter the unique alphanumeric report number(s) assigned by the organization performing the report.

Block 9. Sponsoring/Monitoring Agency Name(s) and Address(es). Self-explanatory.

Block 10. Sponsoring/Monitoring Agency Report Number. *(If known)*

Block 11. Supplementary Notes. Enter information not included elsewhere such as: Prepared in cooperation with...; Trans. of...; To be published in.... When a report is revised, include a statement whether the new report supersedes or supplements the older report.

Block 12a. Distribution/Availability Statement. Denotes public availability or limitations. Cite any availability to the public. Enter additional limitations or special markings in all capitals (e.g. NOFORN, REL, ITAR).

- DOD - See DoDD 5230.24, "Distribution Statements on Technical Documents."
- DOE - See authorities.
- NASA - See Handbook NHB 2200.2.
- NTIS - Leave blank.

Block 12b. Distribution Code.

- DOD - Leave blank.
- DOE - Enter DOE distribution categories from the Standard Distribution for Unclassified Scientific and Technical Reports.
- NASA - Leave blank.
- NTIS - Leave blank.

Block 13. Abstract. Include a brief *(Maximum 200 words)* factual summary of the most significant information contained in the report.

Block 14. Subject Terms. Keywords or phrases identifying major subjects in the report.

Block 15. Number of Pages. Enter the total number of pages.

Block 16. Price Code. Enter appropriate price code *(NTIS only)*.

Blocks 17. - 19. Security Classifications. Self-explanatory. Enter U.S. Security Classification in accordance with U.S. Security Regulations (i.e., UNCLASSIFIED). If form contains classified information, stamp classification on the top and bottom of the page.

Block 20. Limitation of Abstract. This block must be completed to assign a limitation to the abstract. Enter either UL (unlimited) or SAR (same as report). An entry in this block is necessary if the abstract is to be limited. If blank, the abstract is assumed to be unlimited.

Final Report of Research and Development
for the period of April 1, 1991 through September 31, 1991

Titanium Carbide-Graphite Composites

November 8, 1991

For the Competitively Awarded
Contract: DAAL03-91-C-0015

for

US Army Research Office
P. O. Box 12211
Research Triangle Park, NC 27709-2211

by

D. Cummings

Advanced Technology Materials, Inc.
7 Commerce Drive
Danbury, CT 06810

1. Introduction

c. Identification and Significance of the Problem or Opportunity

Ceramic materials are gaining importance in the construction of high efficiency combustion engines. Their high temperature strength and corrosion resistance enable an engine to operate at higher temperatures, thereby improving fuel efficiency. The friction properties and wear resistance also must be satisfactory if ceramic moving components are to be successful. Unfortunately, typical friction coefficients in air for silicon nitride, silicon carbide, alumina, and zirconia are relatively high (1). Wear is often appreciable. This problem is compounded by a lack of suitable liquid lubricants that are effective at the temperatures present in new high efficiency engines. The development of a high temperature solid state lubrication system has the potential of overcoming current limitations with the friction and wear characteristics of ceramics, facilitating their use in more engine components.

One of the materials that has repeatedly been shown to be an effective solid state lubricant is graphite. Cast iron, for example, can show self-lubricating properties when it contains a sufficient quantity of graphite in its microstructure (2). Composites of graphite particulates and aluminum-silicon alloys have also shown admirable friction and wear properties (3). Metal-graphite composite materials are usually produced by casting. Often, particulate graphite is added to the melt.

However, an analogous technique cannot be used for most ceramics. Partially stabilized zirconia and silicon nitride, two materials often considered for high temperature engine applications, are usually prepared via powder routes. Any graphite added would likely react with the matrix material during sintering, decreasing its lubrication value and the strength of the composite.

A refractory carbide, such as titanium carbide, is viewed as an alternative. Titanium carbide is chemically inert, oxidation resistant to 1100°C, and has high hardness. Furthermore, it can be prepared from the melt. The formation of a graphite-titanium carbide composite is straightforward.

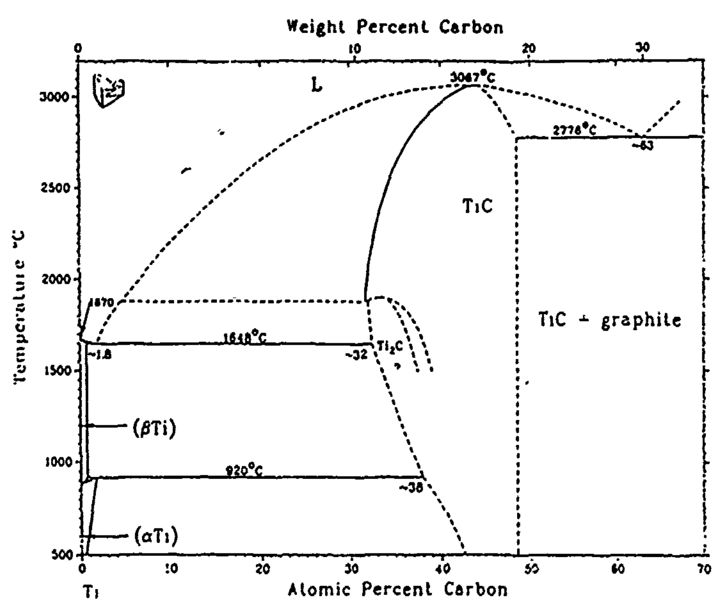

Figure 1
Titanium-Carbon Phase Diagram

Figure 1 shows the titanium-carbon phase diagram. Solidified melts with greater than 48.5 atomic percent of carbon are composite materials containing titanium carbide and graphite. By controlling the thermal environment during solidification, different orientations and sizes of the graphite precipitates can be produced.

Titanium carbide is a very refractory material with a melting temperature of 3067°C. However, pure titanium carbide undergoes a ductile to brittle transition at 800°C (4-6). For those applications that have operating temperatures in excess of 800°C, the loss in hardness and strength would be detrimental to titanium carbide's friction and wear properties. Two ways of increasing titanium carbide's high temperature hardness are the addition of small amounts of boron and the alloying of titanium carbide with vanadium carbide. Figure 2 shows the effect of boron on the critical resolved shear stress as a function of temperature of titanium carbide. Figure 3 shows the effect of vanadium carbide additions on compressive yield strength of titanium carbide as a function of temperature.

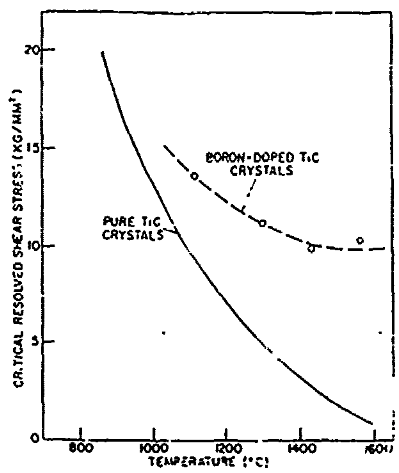

Figure 2
The Effect of Boron on the CRSS of Titanium Carbide (7)

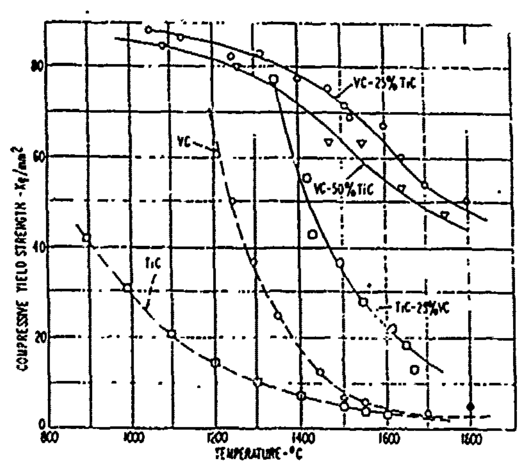

Figure 3
The Effect of Vanadium Carbide on the
Compressive Yield Strength of Titanium Carbide (8)

Titanium carbide is relatively oxidation resistant to 1100°C due to the formation of titanium oxides. These oxides have also been reported to act as a good solid state lubricant (9). A titanium carbide-graphite composite may therefore have good friction and wear properties in both oxidizing and reducing environments.

In summary, titanium carbide-graphite based composites are viewed as having potentially low friction coefficients and low wear rates over a wide range of temperature and atmosphere environments.

2. Phase I Technical Objectives

The objective of this Phase I program was to produce titanium carbide-graphite composites and do a preliminary evaluation of their friction, wear, oxidation, and strength properties. Specific objectives were as follows:

1. The fabrication of titanium carbide-graphite composites.
2. The optical characterization of the microstructure of these composites.
3. The determination of friction coefficients and wear rates for these materials at 25 and 700°C.
4. The identification of the wear mechanism for titanium carbide-graphite composites.
5. An evaluation of the oxidation resistance of titanium carbide-graphite composites at 700°C.
6. The measurement of compressive strength of titanium carbide-graphite composites.

3. Program Technical Results

Task 1: Production of titanium carbide-graphite composites.

Following, is a description of the procedures used for each of the four compositions.

Pure TiC: A conventional float zone geometry was used for this composition. Stoichiometric hot pressed rods of titanium carbide were consumed, from which fully dense ingots of titanium carbide solidified. Both the hot pressed rods and the ingots produced were 0.5 inches in diameter. The ingots were grown at a rate of 0.5 inches per hour. This speed could not be increased due to a thermal cracking problem that was only encountered with this composition. The slow growth rate resulted in the formation of large grains, easily seen without magnification.

TiC/C: A modified float zone method was used for the production of ingots of this material. Hot pressed rods of stoichiometric titanium carbide, 0.75 inches in diameter, were placed inside purified graphite tubes with inside diameters of 0.75 inches. The outside diameter of the graphite was machined down until the weight per inch of the graphite represented 11 percent of the weight per inch of the titanium carbide. The eutectic composition in this system is stoichiometric titanium carbide plus 10 weight percent carbon. Therefore, by controlling the temperature of the melt so that a thin shell of graphite remained unmelted, a eutectic melt was reproducibly created. Figure 4 shows this geometry,

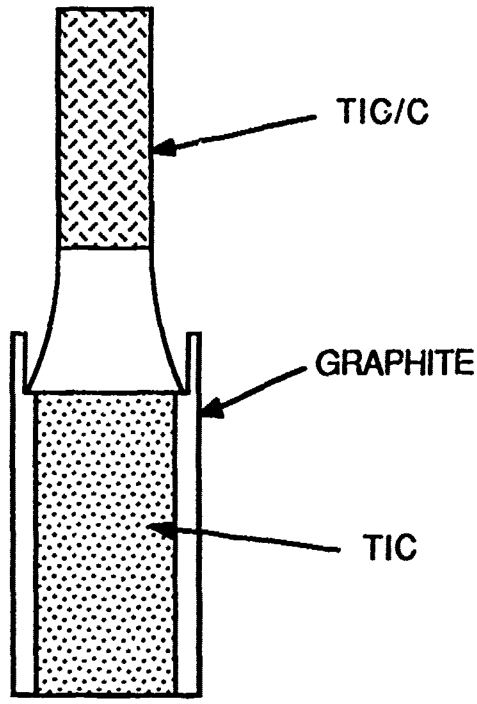

Figure 4
Modified Float Zone Geometry

The TiC/C ingots were grown at a rate of 20 inches per hour. The diameter of the ingots were roughly 0.5 inches in diameter. Cracking did not appear to be a problem.

TiC/B/C: An identical procedure was used for the production of these samples as was used for the TiC/C samples. The one weight percent boron was added by coating the inside of the graphite tubes with boron powder in acetone.

TiC/VC/C: These ingots were produced using a variation of the method used for the previous two compositions. The 25 mole percent vanadium carbide was supplied in the form of vanadium carbide powder placed around a hot pressed 0.5 inch diameter titanium carbide rod and inside a 0.75 inch inner diameter graphite tube. The geometry is shown in Figure 5.

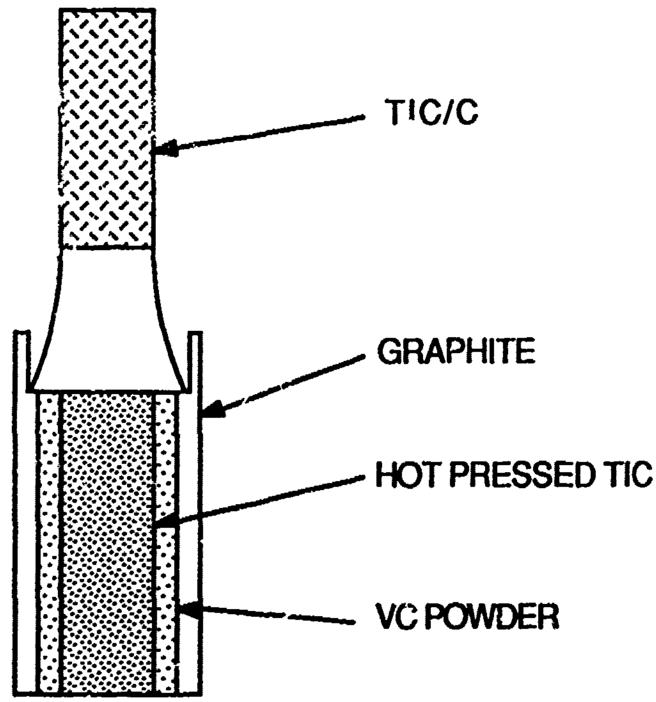

Figure 5
TiC/VC/C Geometry

The eutectic composition in the 3TiC/1VC-carbon system contains roughly five weight percent carbon. It was not practical to machine down the graphite tubes to only five to six weight percent of the carbide. The graphite tubes would be too fragile. Therefore, tubes weighing ten weight percent of the carbide were used, resulting in a difficulty in preventing a composition slightly richer in carbon than the eutectic from forming.

When 0.5 inch diameter ingots of this composition were produced at a growth rate of 20 inches per hour, cracks were found in the ingots. The reason for this was probably the higher yield strength of titanium carbide/vanadium carbide alloys versus titanium carbide alone. Decreasing the diameter of the ingot to 0.32 inches in diameter solved the cracking problem.

Alternate Fabrication Methods

While the float zone techniques that are being used in this Phase I program are effective at producing the desired microstructures for these composites, alternate methods may have economic advantages.

Fabrication methods in which the melt is contained in a crucible of the same composition as the melt represent another alternative. The crucible would be cooled to prevent it from melting. The melt could be created by induction or by radiation.

Task 2: Optical Characterization of Composite Microstructures

Optical and scanning electron micrographs were taken of each of the three composite compositions. These are shown in Figures 6 through 11.

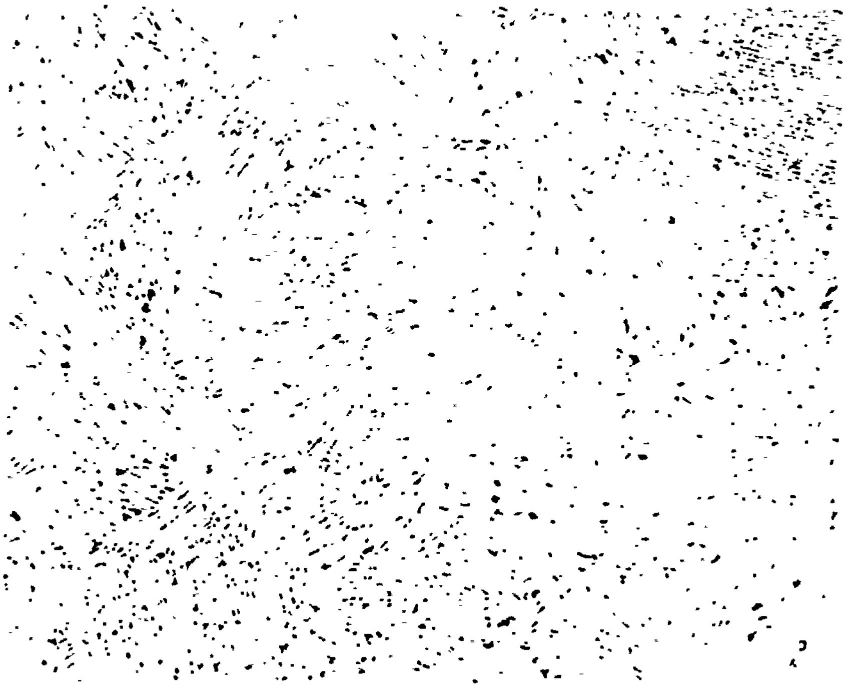

Figure 6
Optical micrograph of TiC/C (200X)

Figure 7
Optical micrograph of TiC/C/B (100X)

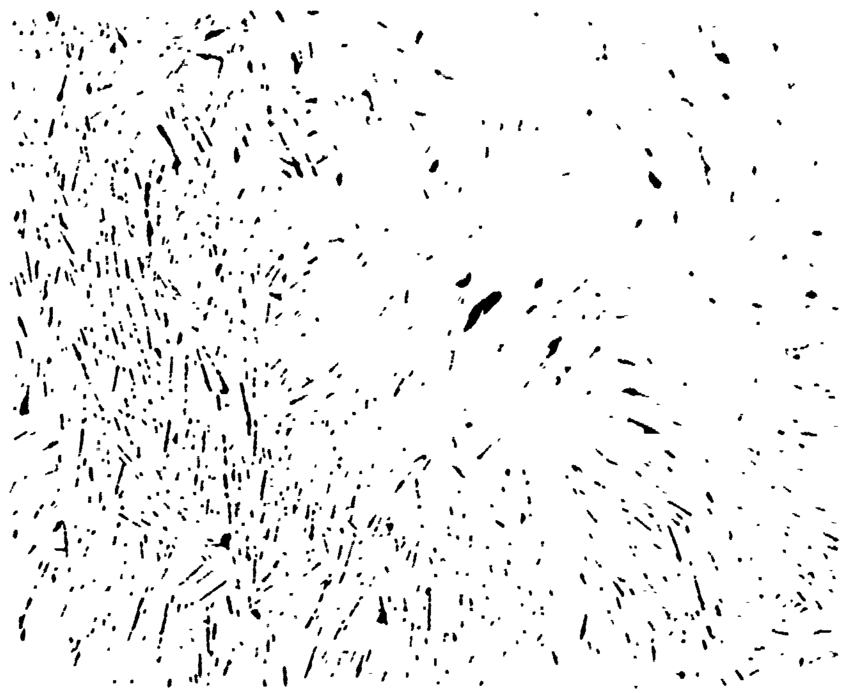

Figure 8
Optical micrograph of TiC/VC/C (100X)

Figure 9
Scanning Electron Micrograph of TiC/C

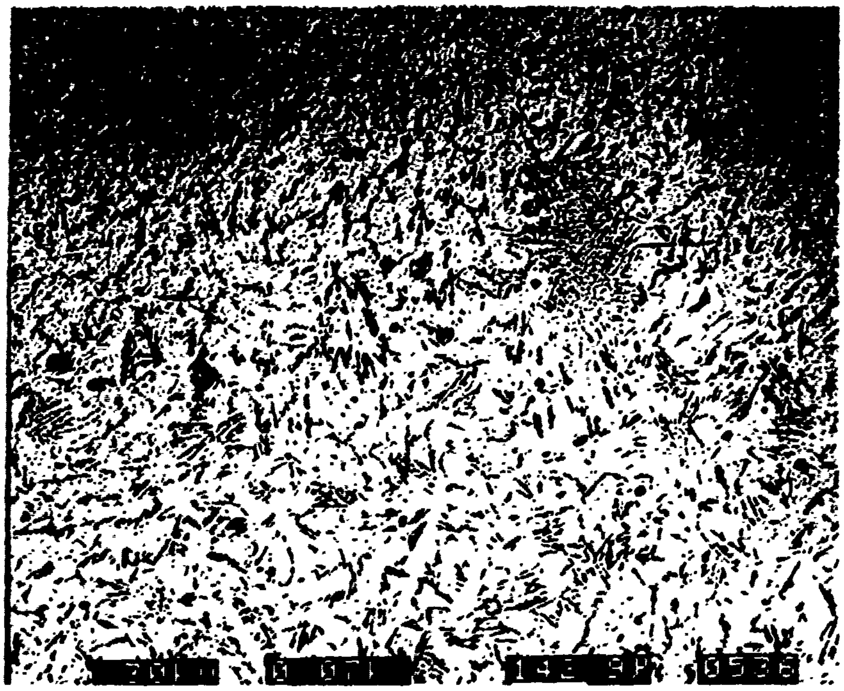

Figure 10
Scanning Electron Micrograph of TiC/C/B

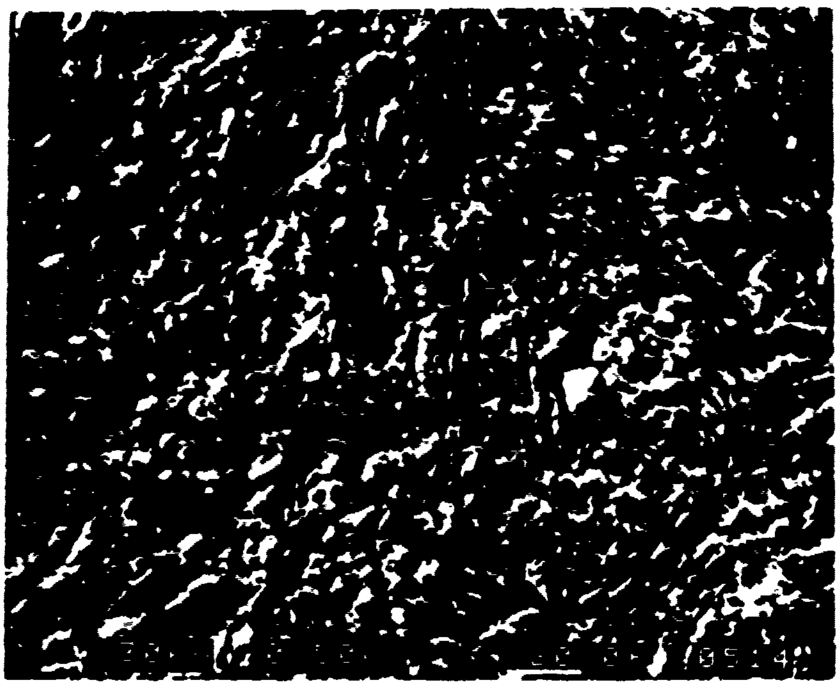

Figure 11
Scanning Electron Micrograph of TiC/VC/C

As these micrographs show, the pure TiC/C had the smallest graphite precipitates. The TiC/C and TiC/VC/C compositions were fairly uniform throughout the ingots. The TiC/C/B had both fine and coarse precipitates. It is not clear why this was the case, since the growth rates were the same for all compositions.

Task 3: Friction and Wear Testing

Friction and wear testing was done at Southwest Research Institute under the direction of Dr. James Lankford. A complete description of this work is included as an Appendix at the end of this report.

Each of the four compositions were tested for friction and wear using a reciprocating 1/4" diameter pin drawn across a 2" long plate of hot pressed titanium carbide. Five newtons of force were used. The reciprocation rate was 3 cycles per second. The pin geometry is shown in Figure 12.

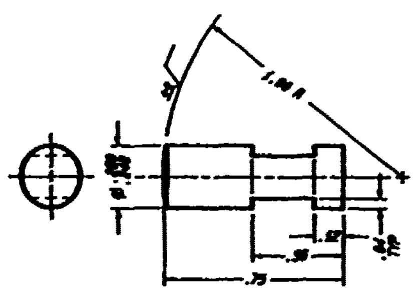

Figure 12
Friction Pin Geometry

The first set of tests performed were of 10,000 cycles in duration, and at temperatures of 22, 600, and 900°C. The raw data from these tests are shown in Figures 13-15. Some observations include:

- Pure titanium carbide exhibited the lowest friction coefficient at 22°C (as low as 0.12).
- The titanium carbide/graphite composite composition with 1% boron exhibited the lowest friction coefficient at 900°C (as low as 0.19).
- The titanium carbide/vanadium carbide/graphite sample mechanically failed during the 900°C test.

For all figures contained in this report, the following labels apply:

T	Pure titanium carbide
TC	Titanium carbide/graphite
TBC	Titanium carbide/graphite/boron
TVC	Titanium carbide/vanadium carbide/graphite

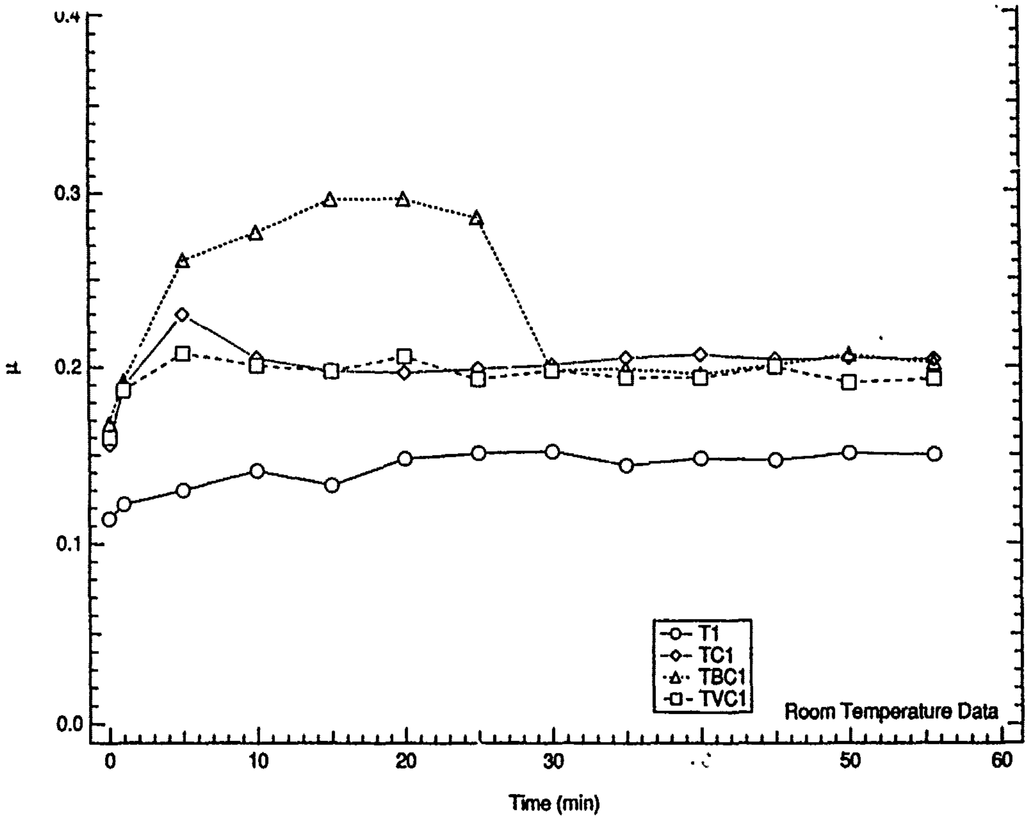

Figure 13
Friction Coefficient Versus Time (23°C)

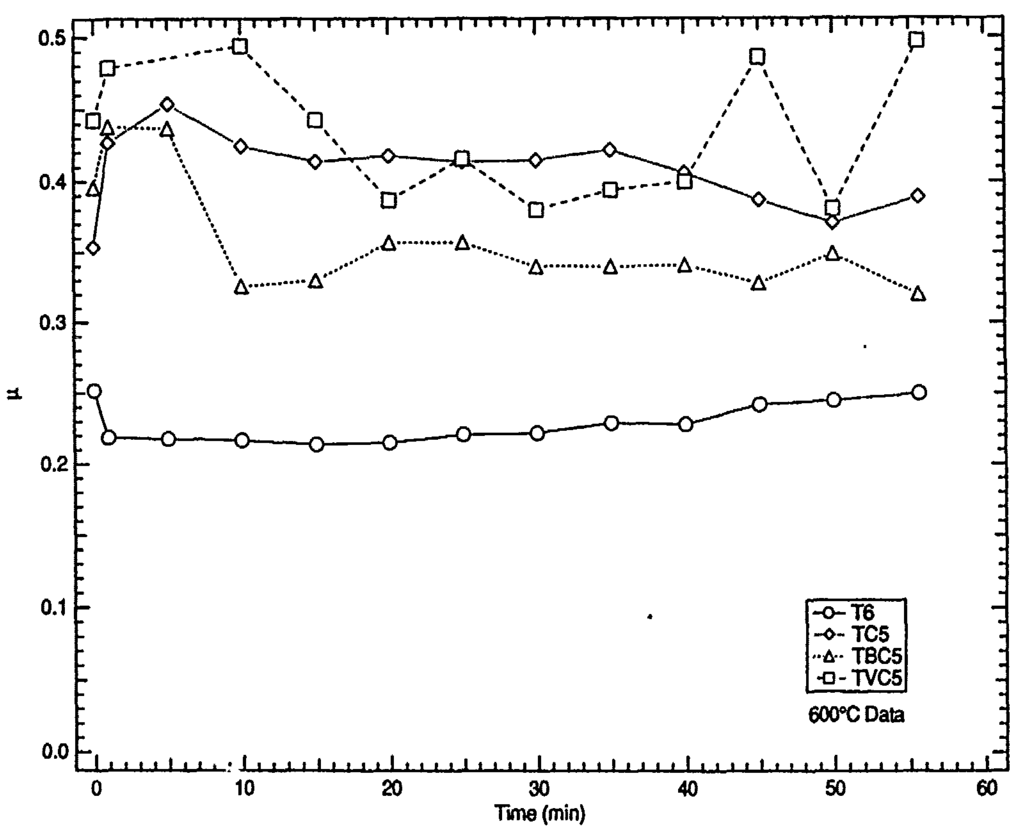

Figure 14
Friction Coefficient Versus Time (600°C)

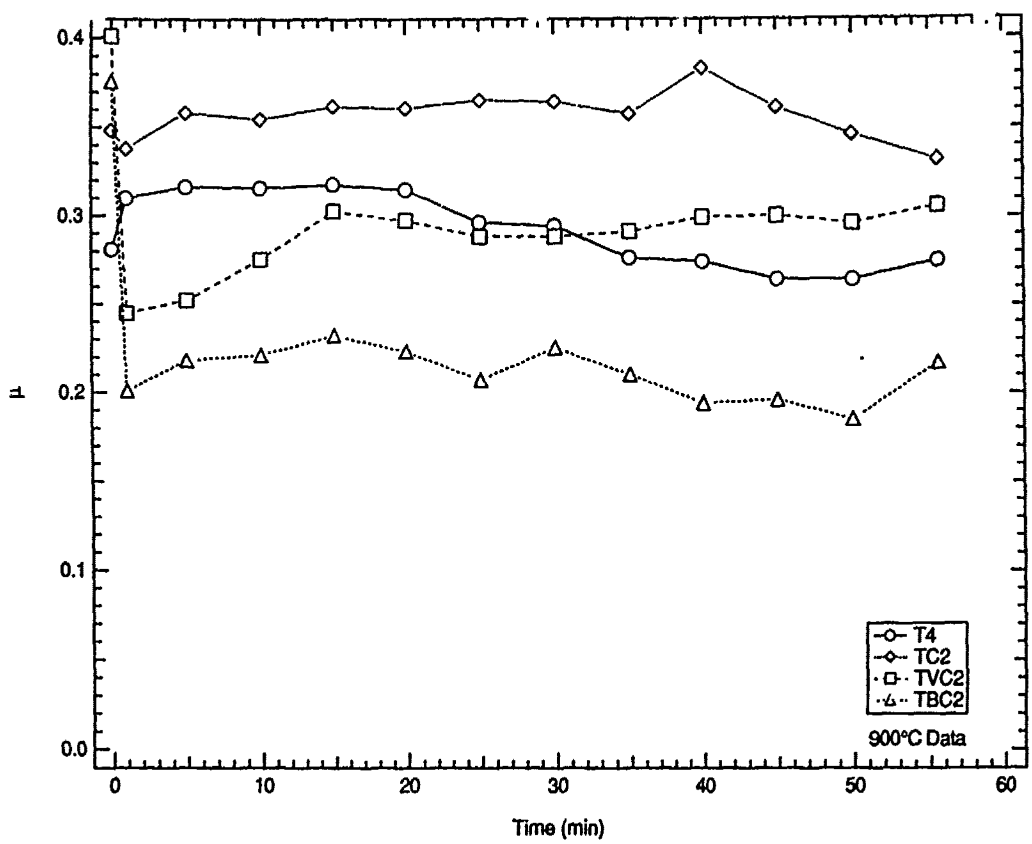

Figure 15
Friction Coefficient Versus Time (900°C)

Wear rates were calculated using the following formula: $K=V/SW$

where

W equals the normal load at the sliding contact
S equals the total distance slid
V equals the volume of material worn away

The data for these calculations can be found in the attached Southwest Research Institute report. Relatively low wear rates were exhibited by all of the samples at 23°C:

Titanium carbide.......................... 3×10^{-6} mm^3/N-m
Titanium carbide/graphite.......................... 5×10^{-6} mm^3/N-m
Titanium carbide/vanadium carbide/graphite.......................... 1×10^{-5} mm^3/N-m
Titanium carbide/boron/graphite..........................$<8 \times 10^{-7}$ mm^3/N-m

High wear rates were exhibited by all compositions at 600 and 900°C. The lowest value was obtained with titanium carbide/vanadium carbide/graphite at 600°C. It had a wear rate of 2×10^{-5} mm^3/N-m.

Originally, the plan was to repeat these tests for durations of 100 and 1000 cycles to better understand the wear mechanism, and how it may change with time. After looking at the initial data, it was determined that more could be learned by conducting tests where temperature was a variable. For example, a test in which the friction coefficient would be measured as the temperature was being raised from 25 to 800°C, then back down to 25°C. This would indicate friction coefficients over a range of temperatures, and indicate if the low temperature friction coefficients are affected by an 800°C heat treatment. For example, the friction coefficient at room temperature may be lowered by oxides that are formed during the high temperature portion of the test. On the other hand, the friction coefficient at room temperature may be increased if graphite is oxidized away during the high temperature portion of the test.

Figures 16-19 show how the friction coefficients varied as the samples were raised from room temperature to 800°C, then back to room temperature (the TiC-VC-C sample was only taken to 600°C). As these figures show, the friction coefficients are generally higher during cool down versus during heat up. This may be indicative of graphite oxidation. The pure titanium carbide sample, however, had a tendency towards lower friction coefficients during cool down, possibly due to titanium oxides being present. The fact that the titanium carbide's friction coefficient remained below 0.31 during cool down from 600°C was noteworthy.

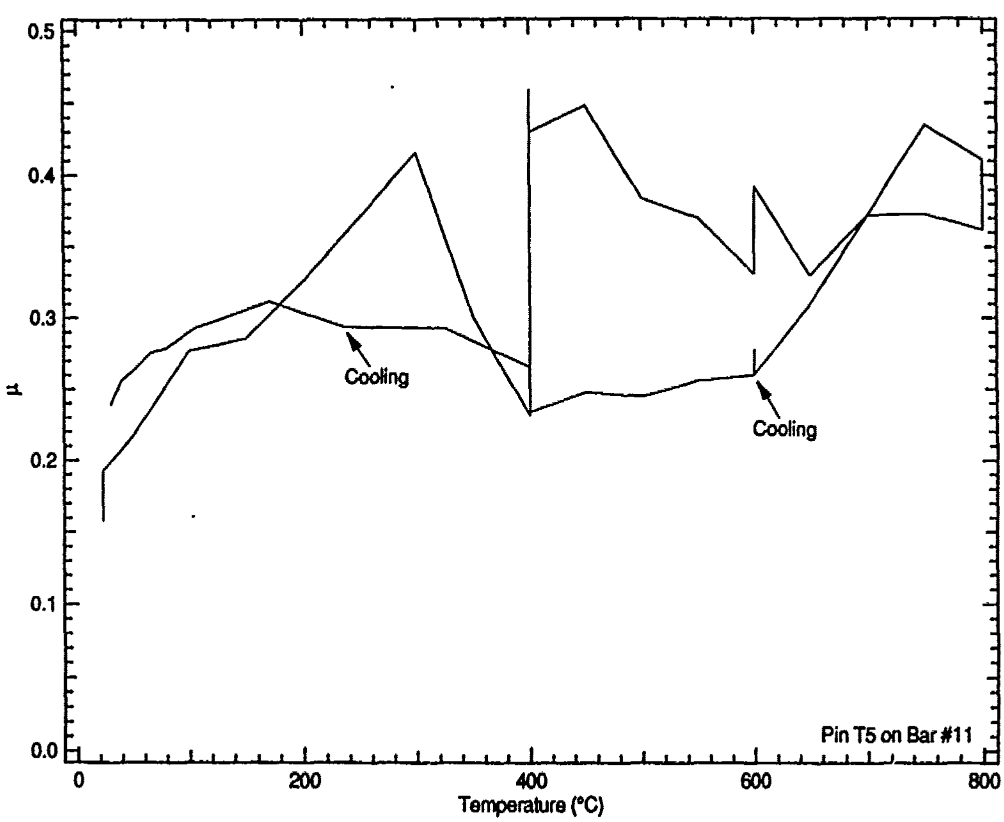

Figure 16
Friction Coefficient Versus Cyclic Temperature for Titanium Carbide

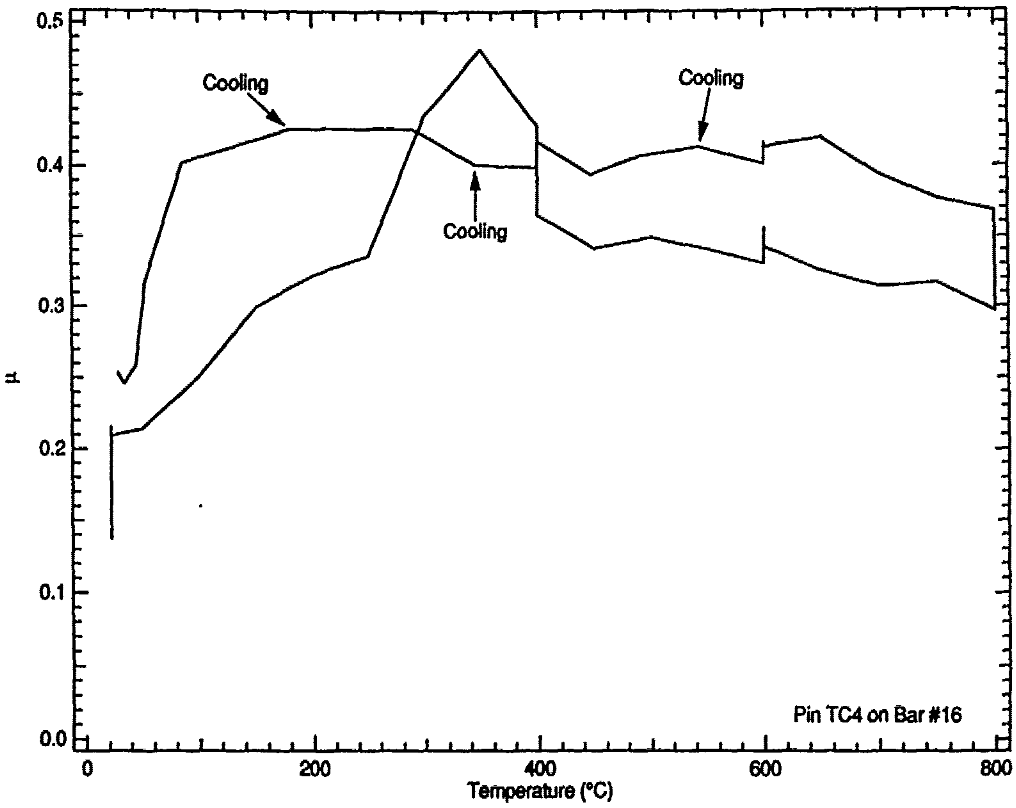

Figure 17
Friction Coefficient Versus Cyclic Temperature for Titanium Carbide/Graphite

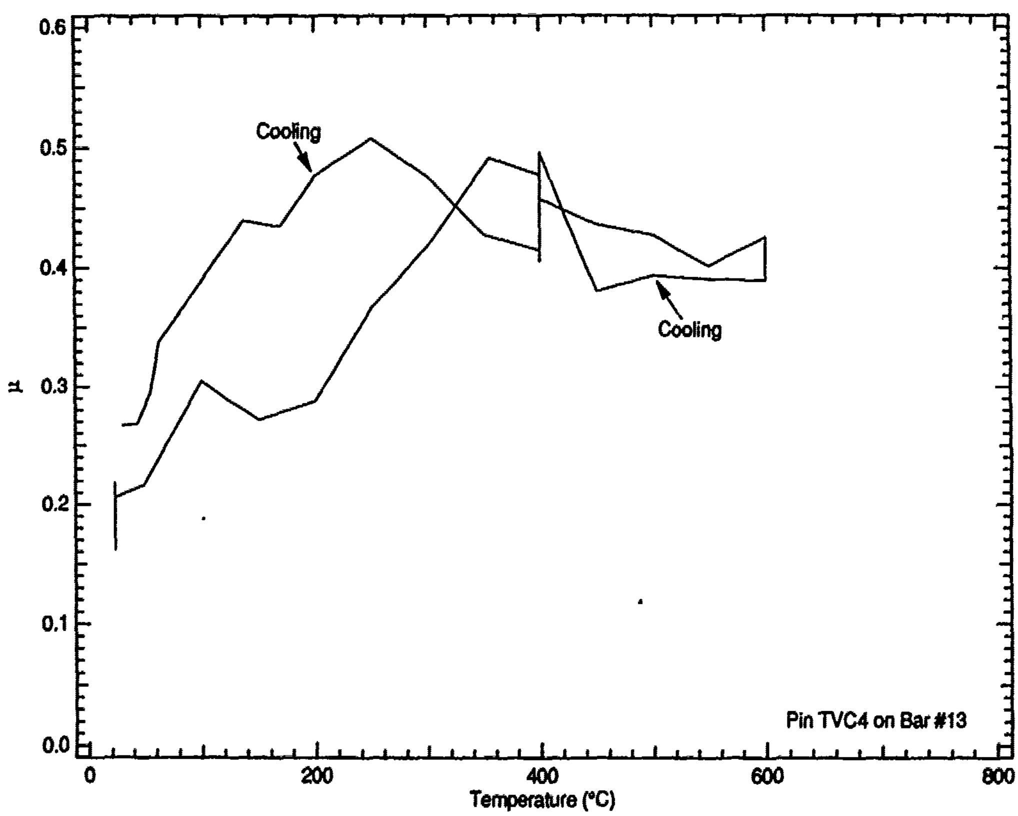

Figure 18
Friction Coefficient Versus Cyclic Temperature for Titanium Carbide/Vanadium Carbide/Graphite

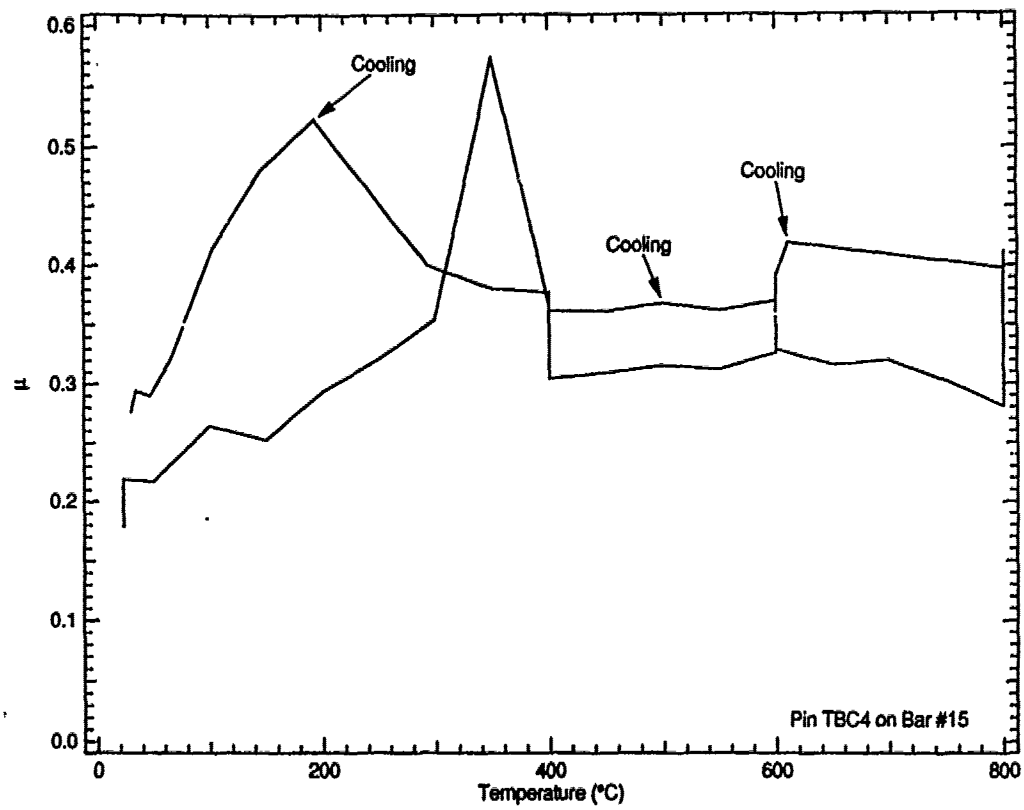

Figure 19
Friction Coefficient Versus Cyclic Temperature for
Titanium Carbide/Boron/Graphite

<u>Task 4</u> SEM analysis of Friction and Wear Test Samples

A representative sample from each of the three temperatures at which 10,000 cycle tests were run was examined by SEM/EDS. Micrographs are included in the attached Southwest Research Institute Report.

The titanium carbide/boron/graphite pin and matching wear plate was examined after the 23°C, 10,000 cycle test. Wear on both the pin and the flat was negligible. Wear debris consisted of titanium and oxygen (boron could not be detected by EDS). This may be indicative of high local temperatures during the test.

The titanium carbide/vanadium carbide/graphite pin and matching wear plate exhibited moderate wear after the 600°C, 10,000 cycle test. The titanium carbide flat appeared to oxidize more than the pin.

Both the titanium carbide and titanium carbide/boron/graphite pins and wear plates were examined after the 900°C test. Significant wear of pins and flats occurred. The pure titanium carbide pin produced subsurface microfracture and cracks in the wear track on the flat. The pin containing boron and graphite had a smooth and glazed wear track

Task 5 Compressive Strength Testing

The values as reported by Southwest Research Institute are as follows. The second value in each table refers to the stress at failure as determined by acoustic emission.

Titanium carbide/graphite:

Spec. No.	σ_{μ}(MPa)	σ_{AE} (Mpa)
1	1642	1174
2	1821	1159
3	1916	1191

Titanium carbide/vanadium carbide/graphite:

Spec. No.	σ_{μ}(MPa)	σ_{AE} (Mpa)
1	1086	902
2	742	614
3	1309	860

Titanium carbide/boron/graphite:

Spec. No.	σ_{μ}(MPa)	σ_{AE} (Mpa)
1	822	610
2	897	700
3	1013	859

This data indicates an inverse relationship between precipitate size and compressive strength. Processing changes could improve compressive strength by decreasing precipitate size.

3. Technical Feasibility

This program showed that titanium carbide based materials can give friction and wear behavior that is highly competitive with other ceramic materials now being considered for friction and wear applications (see Figure 20). This was shown in spite of the fact that only a few of many possible compositions were tried.

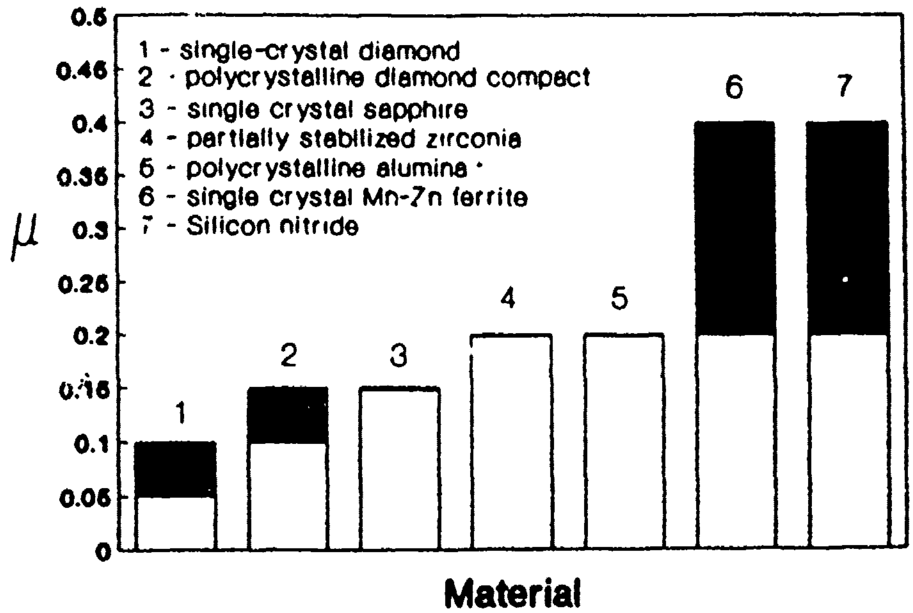

Figure 20
Friction Coefficients of various Materials in Contact with Themselves (10)

The approach of putting graphite precipitates into refractory carbide matrices did not lower friction and wear under the conditions tested. However, changing the load, the sliding speed of the friction couple, the material of the wear flat, or the atmosphere under which the test is conducted could greatly affect the results. Under the test conditions of this program it appears that the grain refinement caused by the presence of graphite precipitates may have increased the friction coefficients at low temperatures. Grain boundary areas have higher surface energy which can translate into higher friction behavior (see Figure 21). Therefore, it is quite conceivable that fine grained pure titanium carbide would have friction and wear behavior that would be inferior to any of the compositions tested in this Phase I program.

Another composition that can easily be prepared from a melt and which could possibly provide a lower friction coefficient under this Phase I program's conditions would be a titanium carbide/titanium diboride composite. Titanium diboride semicoherent precipitates can be formed in single crystal titanium carbide. The benefits of boron oxide high temperature lubrication could be obtained without significantly increasing the material's surface energy.

Compositions that include nitrogen may have titanium nitride or boron nitride phases, both of which could have a favorable impact on the friction and wear behavior of the composite. Titanium carbide/titanium nitride solid solutions can be formed.

The compressive strength of the titanium carbide composites tested was not exceptional, but was certainly adequate for most applications. Grain and precipitate size optimization could greatly affect the numbers obtained.

The oxidation resistance of titanium carbide appeared to be sufficient during the Phase I tests. The addition of more boron could further improve oxidation resistance.

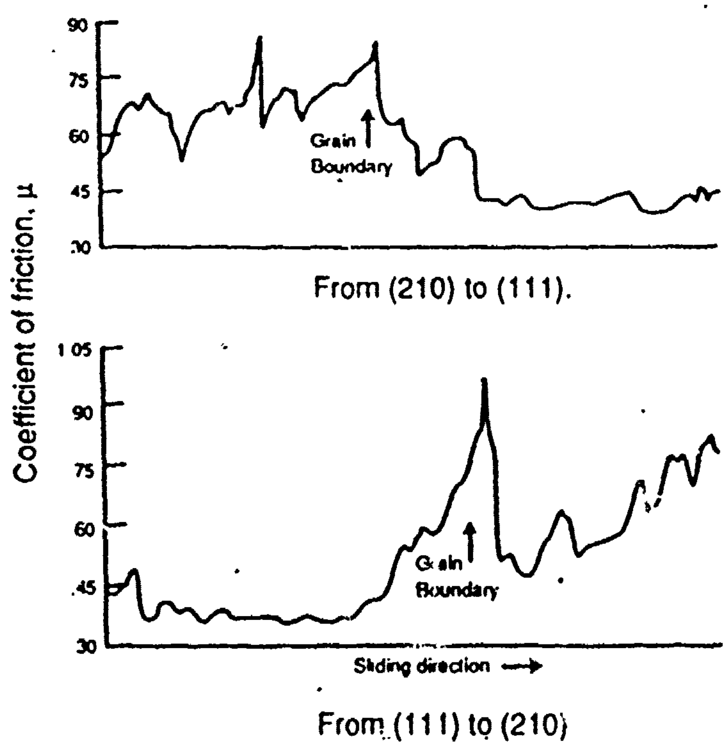

Figure 21
The Friction Coefficient of Single Crystal Copper Sliding Against Polycrystalline Copper (10)

In summary, titanium carbide based materials offer a great deal of flexibility in terms of possible composite compositions, all of which can be prepared from a melt. Further development in this area would entail selecting a specific application and performing friction and wear tests to optimize behavior under those load, atmosphere, and sliding speed conditions.

5. Point of Contact

Report Prepared by:

Del Cummings
Advanced Technology Materials, Inc.
7 Commerce Drive
Danbury, CT 06810
(203) 794-1100

References

1. K. Kato, "Tribology of Ceramics," *Wear*, 136 (1990) 117-133.
2. S. C. Lee, et. al., "The Effect of Graphite Addition on the Friction and Wear of Sintered Cast Iron Fibers," *Scripta Metallurgia*, 22 (1988) 653-658.
3. S. Das, S. V. Prasad, and T. R. Ramachandran, "Microstructure and Wear of Cast (Al-Si Alloy)-Graphite Composites," *Wear*, 133 (1989) 17[illegible]-187.
4. W. S. Williams, "Physics of Transition Metal Carbides," *Materials Science and Engineering*, A105/106 (1988) 1-10.
5. G. E. Hollox, "Microstructure and Mechanical Behavior of Carbides," *Materials Science and Engineering*, 3 (1968/69) 121-137.
6. D. K. Chatterjee, et. al. "Deformation Behavior of Single Crystals of Titanium Carbide," *Journal of Materials Science*, 14 (1979) 2151-2156.
7. W. S. Williams, "Dispersion Hardening of Titanium Carbide by Boron Doping," *Transactions of the Metallurgical Society of AIME*, 2[illegible]3 (1966) 211-215.
8. G. E. Hollox, et. al., "High Temperature TiC-VC Structural Materials," U.S. Patent #3,661,599 May 9, 1972.
9. W. Wei, J. Lankford, and R. Kossowsky, "Friction and Wear of Ion -beam-modified Ceramics for use in High Temperature Adiabatic Engines," *Materials Science and Engineering*, 90 (1987) 307-315.
10. S. Chandrasekar and B. Bhushan, "Friction and Wear of Ceramics for Magnetic Recording Applications-Part I: A Review," *Journal of Tribology*, 112 (1990) 1-13.

SOUTHWEST RESEARCH INSTITUTE

6220 CULEBRA ROAD • POST OFFICE DRAWER 28510 • SAN ANTONIO, TEXAS, USA 78228-0510 • (512) 684-5111 • TELEX 244846

Materials & Mechanics Department
October 29, 1991

Mr. Del Cummings
Advanced Technology Materials, Inc.
520-B Danbury Road
New Milford, CT 06776

Subject: SwRI Project 06-4431
"Evaluation of Titanium Carbide/Graphite Composites"
FINAL REPORT

Dear Del:

This letter constitutes our formal final report on the above referenced project. Work performed included friction and wear testing of several TiC-based ceramic composites, as well as compression testing of three of the materials. The bulk of the results, in graphical and tabular form, are included in a series of Appendices, with the body of the report devoted to a description of the test procedures, followed by a summary and critical discussion of the results.

Experimental Procedures

Materials for testing were provided by the sponsor in the form of pins and flats for reciprocating pin-or-disk testing, and cylindrical specimens for compression testing. Flats were composed of hot-pressed TiC carbide (T), while pins consisted of TiC; TiC/graphite (TC); TiC/VC/graphite (TVC); and TiC/B/graphite (TBC). Compression specimens were composed of TC, TVC, or TBC.

Baseline friction and wear tests were performed at a frequency of 3 Hz, using a load on the pin of 5N, and at temperatures of 23, 600, or 900°C for 10,000 cycles. Severe microcracking problems were encountered with TVC at 900°C, but successful elevated temperature runs were accomplished at 600°C. In addition to these tests, a series of experiments were performed in which temperature was ramped up in 200°C increments, with the friction coefficient established over 30 minutes at 23, 200, 400, 600, and 800°C, followed by a reversal of the sequence back to room temperature.

During the experimental runs, the friction coefficient (μ) was monitored continuously. Data suitable for computing wear rates was generated by profilometry of baseline wear tracks at the end of the test period. Thus, representative wear in the flat can be computed in terms of the profilometry-derived wear cross-section, the length of the wear track (12 cm), and the density of the TiC.

After testing, selected pins and flats were characterized by scanning electron microscopy (SEM) and energy dispersive spectroscopy (EDS). It should be noted that due to its low atomic number, B cannot be detected by means of EDS.

All compression tests were performed under ambient conditions at a strain rate of 3.3 x $10^{-5}s^{-1}$. High strength alumina platens were used to transfer the load from the ram to the samples. Acoustic emission was used to monitor the onset of microfracture leading to eventual failure.

Discussion of Results

The effect of temperature (T) on the friction coefficient (μ) of each material is summarized in Figures 1 - 3 for T = 23, 600, and 900°C, respectively. From ambient conditions to 600°C, the lowest values of μ (0.15 - 0.21) are obtained for case T, i.e., TiC pin on TiC flat. However, at 900°C (Figure 3), TBC is superior, with an average friction coefficient of about 0.2.

The relative reversibility of μ during heating and cooling is shown for each pin material in Figures 4 - 7. The results indicate that μ(T) is essentially reversible for each material.

Wear behavior on flats (see profilometry within Appendices) with a few exceptions, supported the friction results. In particular, at 23°C, very low wear was observed for T, in agreement with its low μ value. However, TBC exhibited basically no wear at 23°C, and wear of TC was barely visible.

At 600°C, flat wear was heavy for all couples, with the exception of TVC. Rather surprisingly, this material (at this temperature) had the highest friction coefficient (Figure 2).

Finally, at 900°C the best (flat) wear resistance was obtained using T pins. The TVC material virtually disintegrated at this temperature.

SEM/EDS work (Appendices) performed on some of the pins and flats provides some insight as to operative wear mechanisms. Elevated temperature response was emphasized, although a representative ambient case was characterized.

In the latter instance, TBC was considered. It was found that the wear spot on the pin was exceptionally small, commensurate with the essentially unmeasurable wear measured on the flat. Areas with and without the spot, including debris from the pin, were determined by EDS to consist of Ti and O; as noted earlier, the EDS system will not detect B. The presence of considerable oxygen outside, but near the wear spot, suggests the generation of high local temperatures.

At 600°C, TVC pins had a surprisingly large wear spot and associated volume of debris, considering the relatively moderate flat wear. Cracking, possibly of oxide layers, was observed within the wear spot on the pin; no such cracking was observed on the wear track of the mating flat. Spectroscopy indicated V depletion within the wear spot itself, but V was adjacent to the spot and with the associated debris. Titanium and either O or V were found on the wear spot and in the debris, but no oxygen was detected on the pin away from the spot. This suggests that the O/V uncertainty probably involved V, and that O was not present. In the case of the mating flat, some Ti and O was observed in the debris; it thus appears that the flat oxidized, and that the pin may not have done so.

At 900°C, the T pins exhibited both wear, wear debris, and cracking. The same was observed for the mating flats; in all instances (within and without wear spot and wear tracks) the material consisted of oxidized Ti. The path of the cracks, oriented normal to the diversion of pin motion, was unaffected by the presence of oxide particles. The material in the (flat) wear track seems to fail by subsurface microfracture with subsequent delamination of oxide particles.

Also at 900°C, TBC exhibited pin and flat wear with associated debris; everywhere the apparent chemistry was oxidized titanium (B probably was present in pin debris). No cracking in either pin or flat was observed, and the oxide layers on the flats were smooth and glazed in appearance. They apparently fail by subsurface delamination, accounting for the measured wear.

Summary

A number of interesting data have been obtained, but results are not conclusive in favor of the composite approach which was implemented. In the future, it would be helpful to fabricate the flats in the composite form, rather than the pins, to facilitate lubrication via oxide transfer from substrate to pin, rather than vice versa.

The graphite component apparently provided little lubrication per se, probably because the graphite particles were not preferentially oriented for sliding parallel to the pin motion. On the other hand, the apparent lack of oxidation of the TVC material was puzzling, and may deserve further study—wear of TVC at 600°C was extremely low, despite its friction coefficient of ~ 0.4.

I hope you find this report informative and helpful in your efforts to obtain Phase II support. I have appreciated this opportunity to support your materials development program, and look forward to further collaboration. Please call me should you have any questions.

Yours sincerely,

James Lankford
Institute Scientist

JL:llr
D:\MS\LANKFORD\M431FR.DOC

cc: G. R. Leverant
U. S. Lindholm
B. J. Andrews

APPROVED:

Gerald R. Leverant, Director
Materials & Mechanics Department

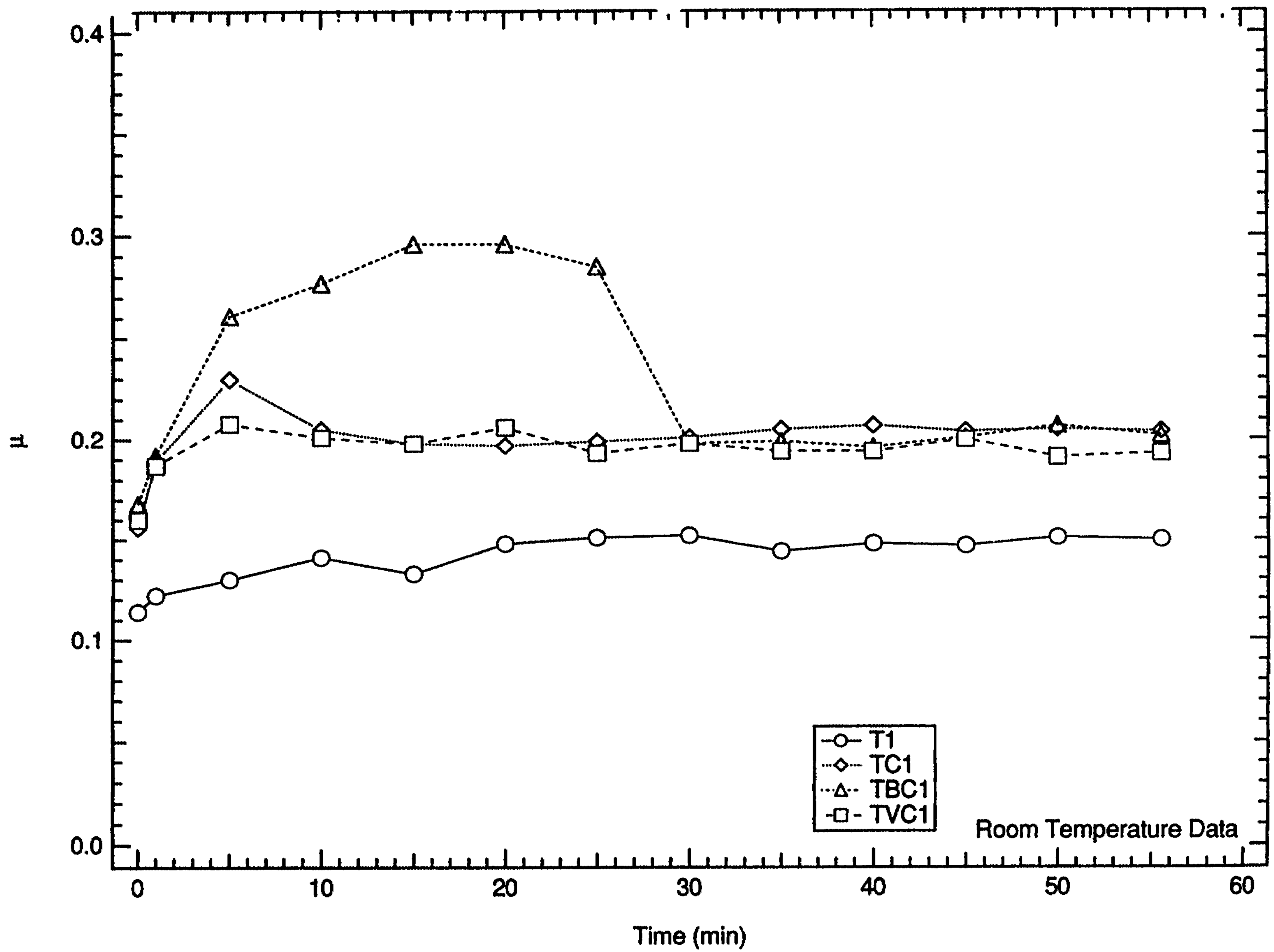

Figure 1. Friction coefficient versus time, 23°C.

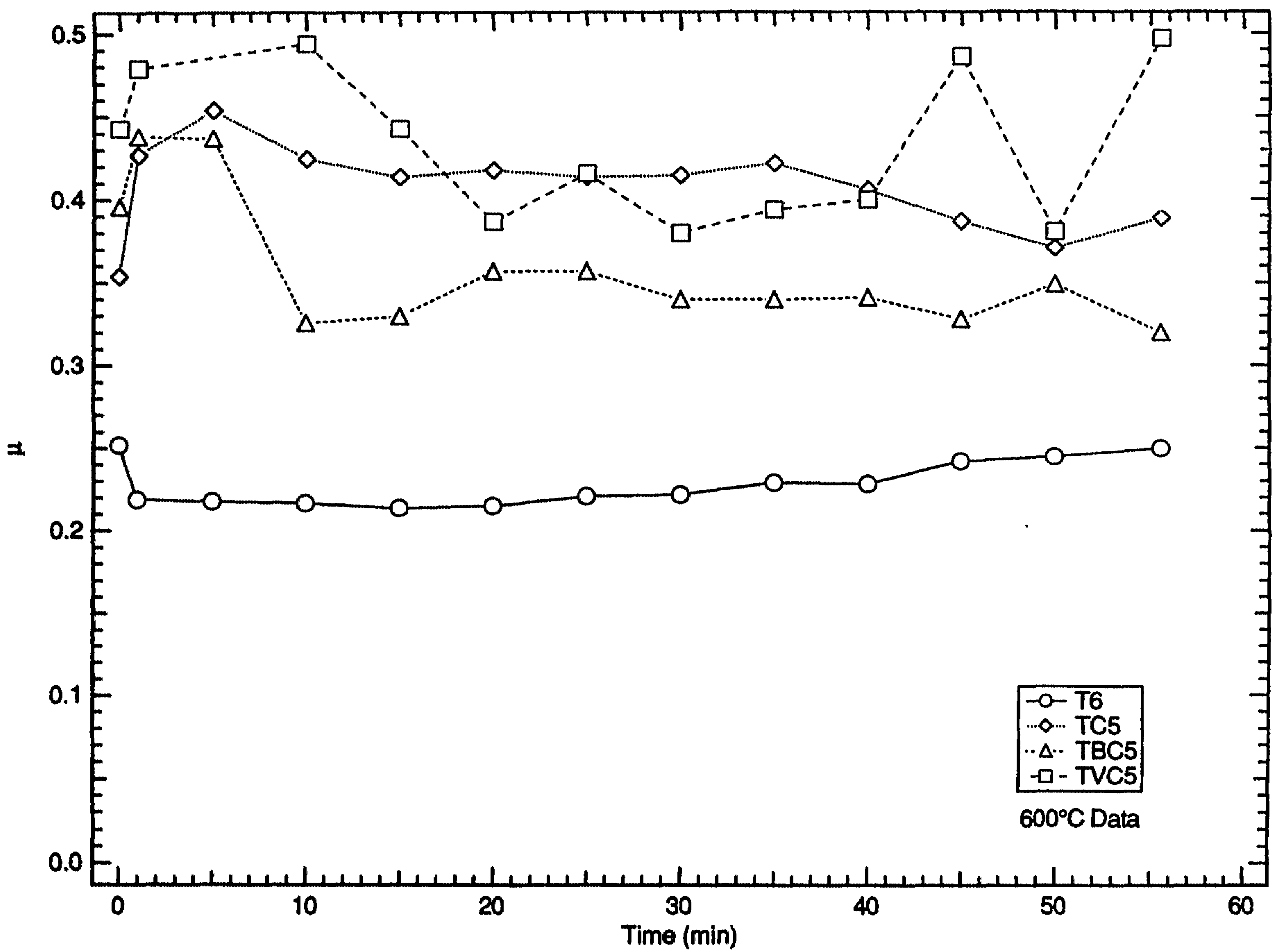

Figure 2. Friction coefficient versus time, 600°C.

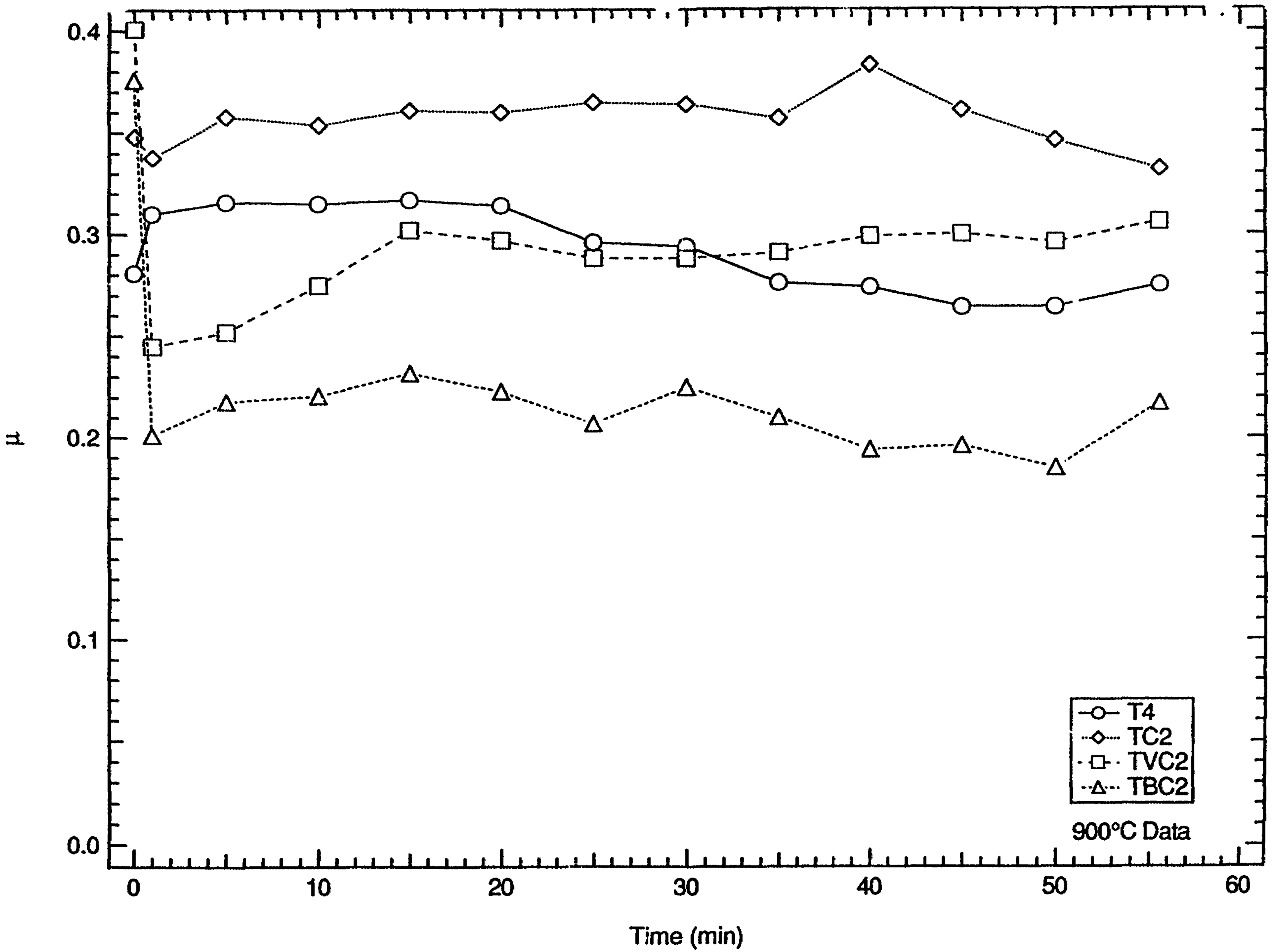

Figure 3. Friction coefficient versus time, 900°C.

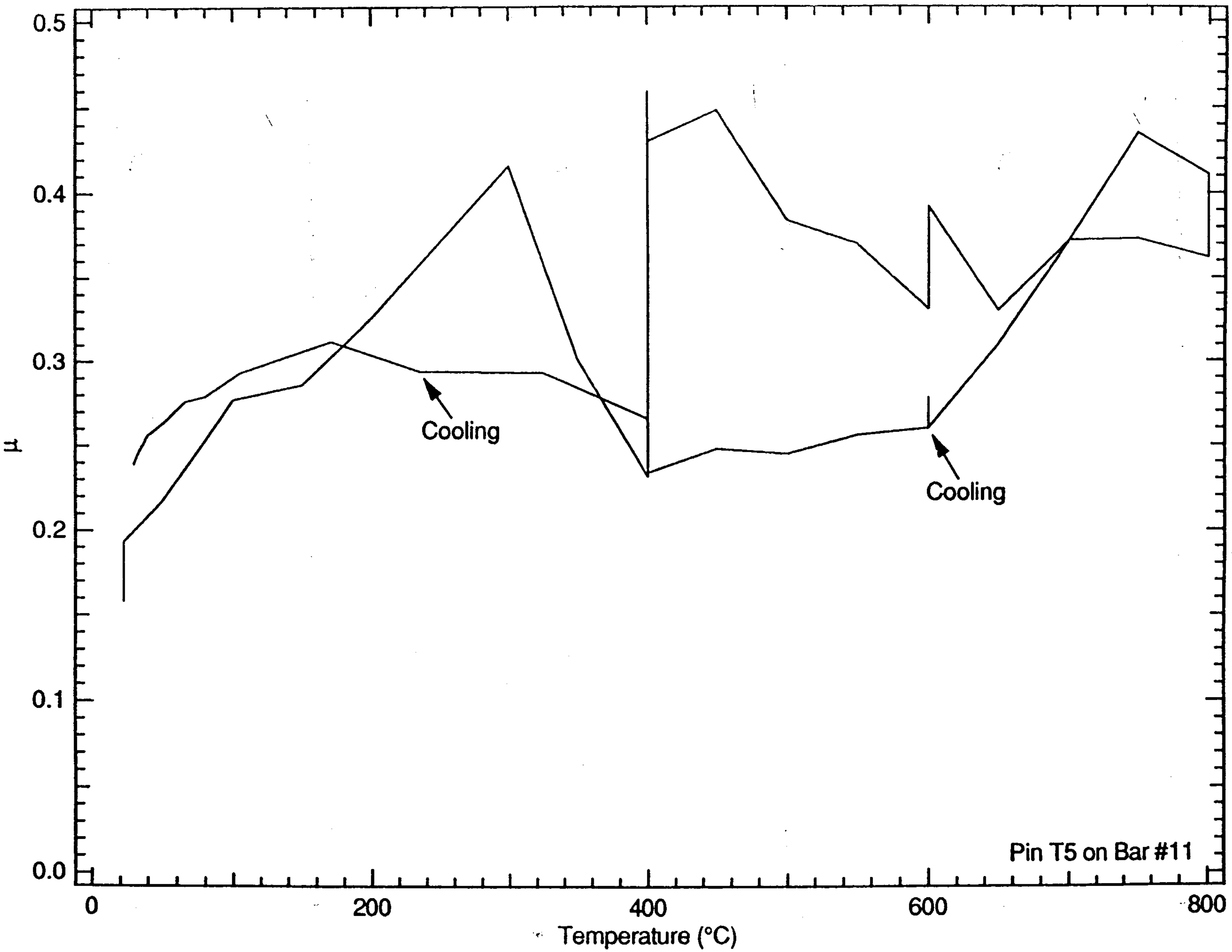

Figure 4. Friction coefficient versus cyclic temperature, T.

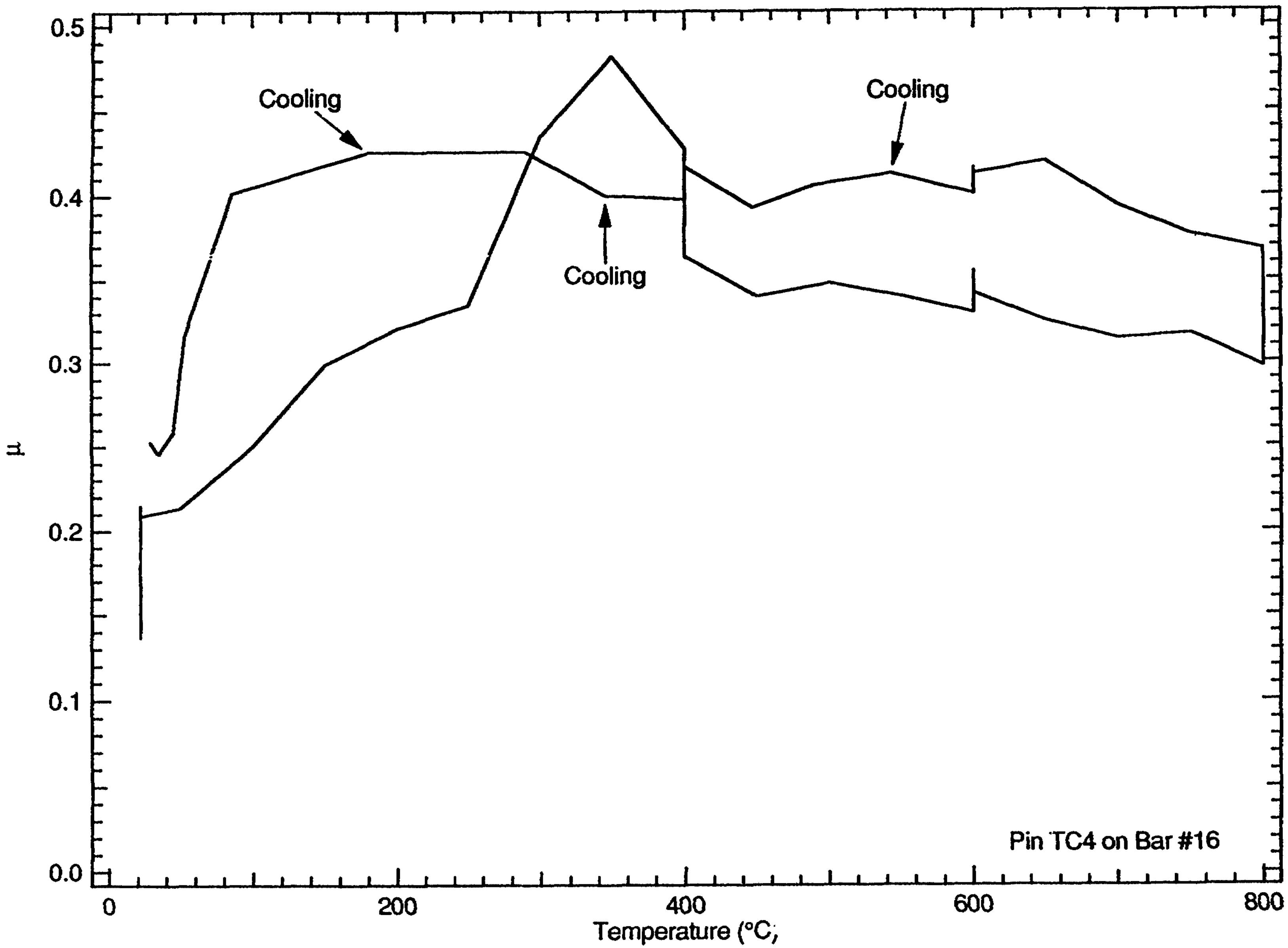

Figure 5. Friction coefficient ver. cyclic temperature, TC.

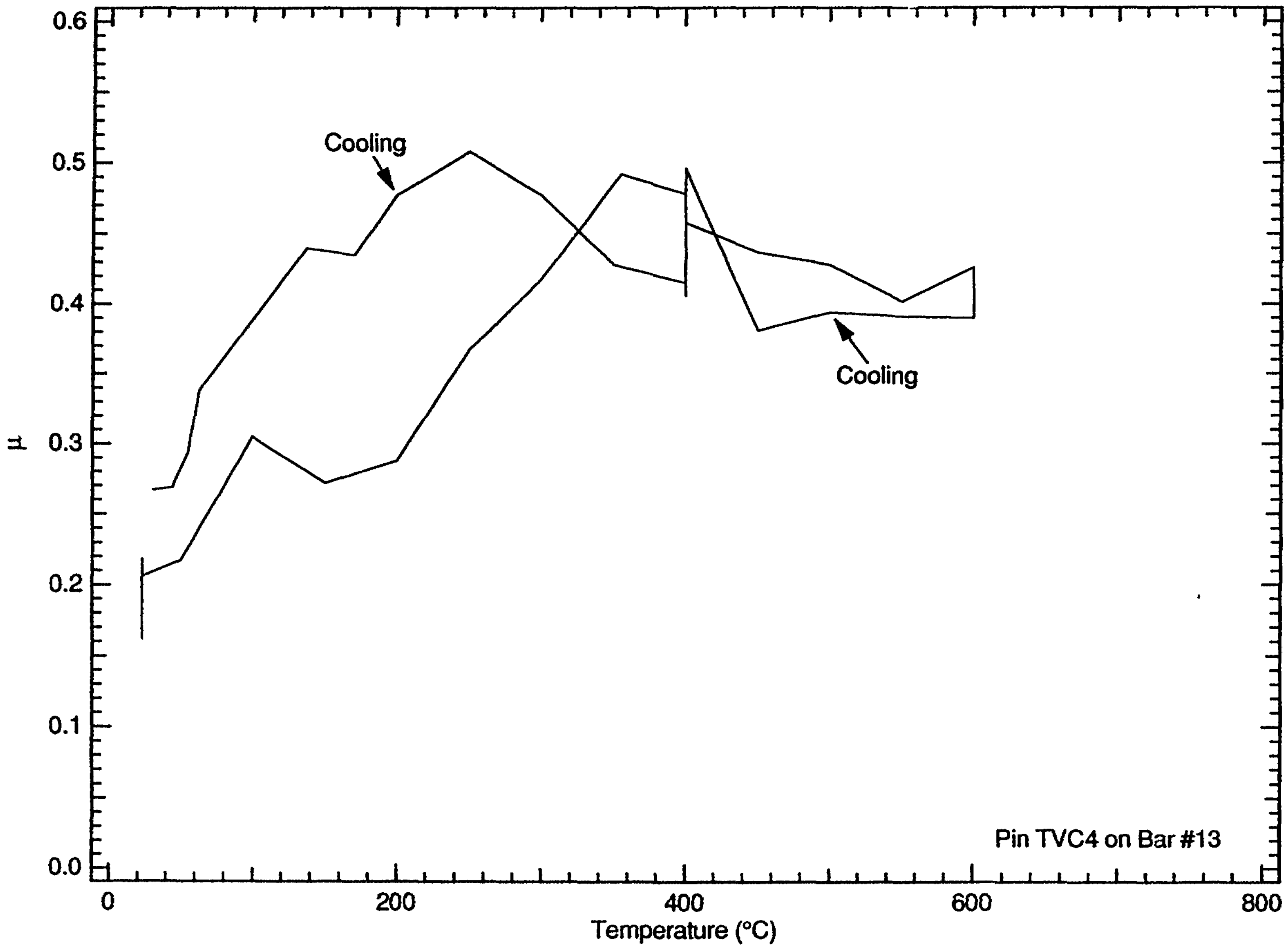

Figure 6. Friction coefficient versus cyclic temperature, TVC.

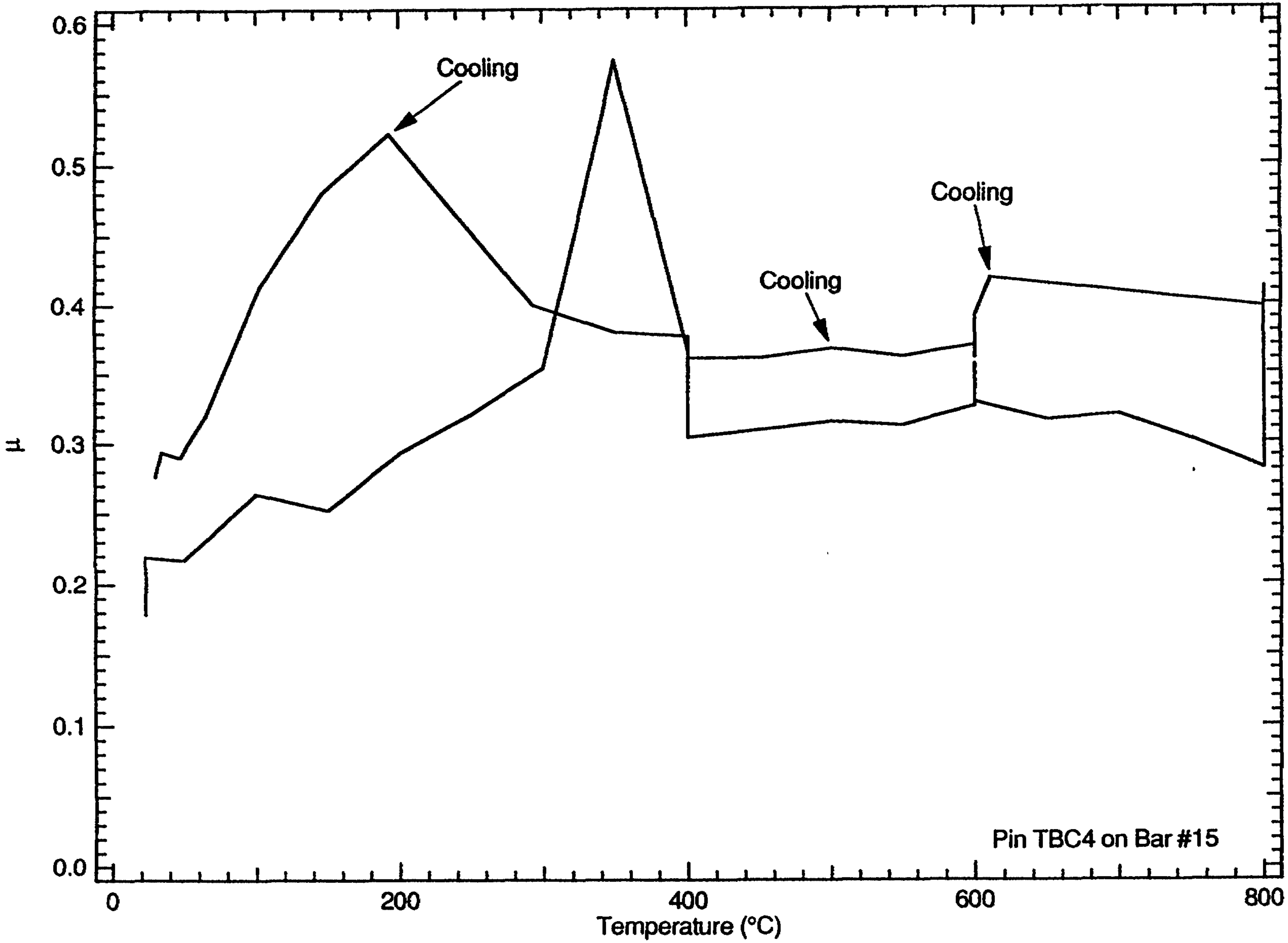

Figure 7. Friction coefficient versus cyclic temperature, TBC.

PIN MATERIAL T
23°C

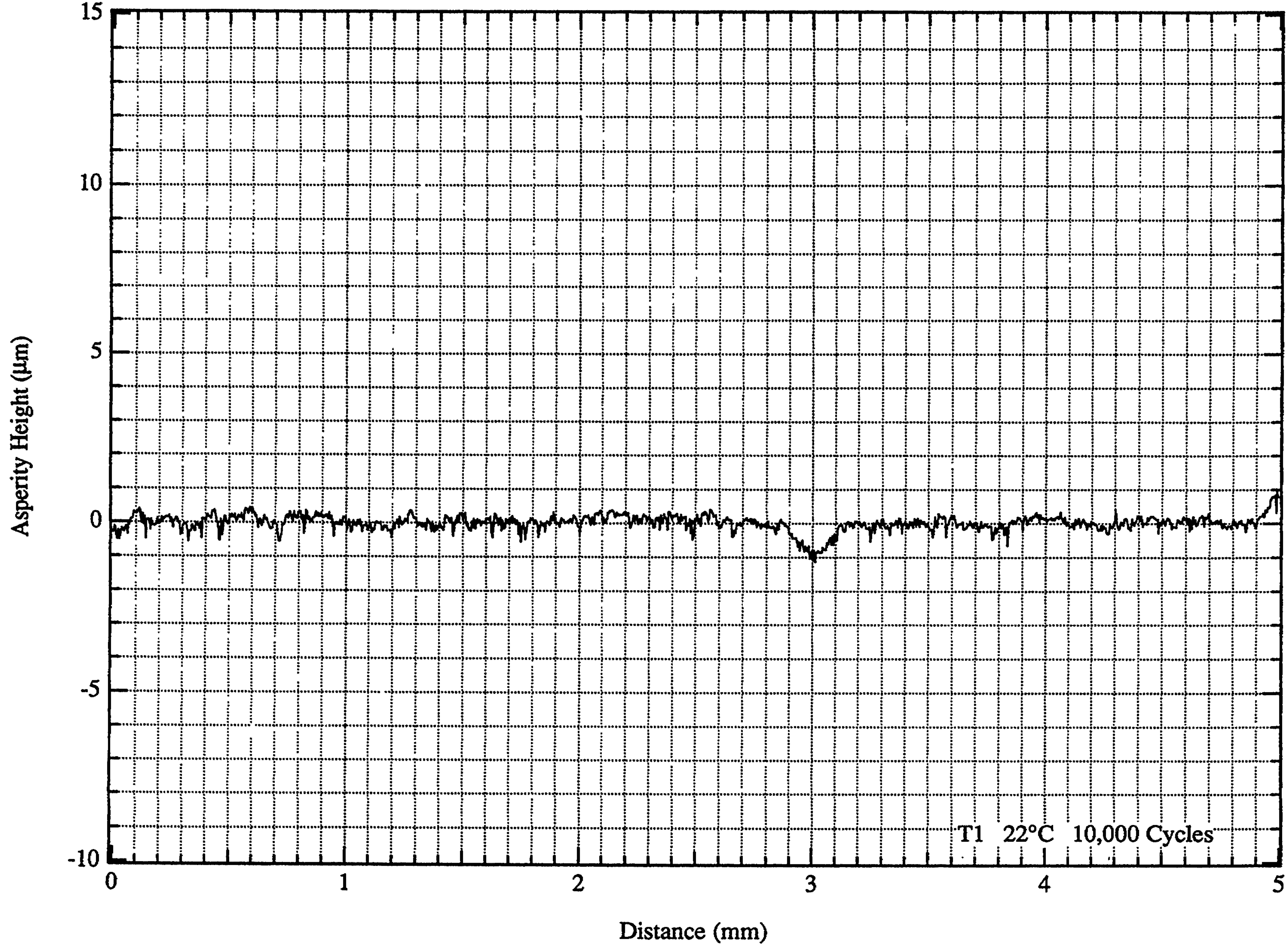

15
10
5
0
-5
-10
Asperity Height (µm)
0
1
2
3
4
5
Distance (mm)
T1 22°C 10,000 Cycles

MATERIAL T
600°C

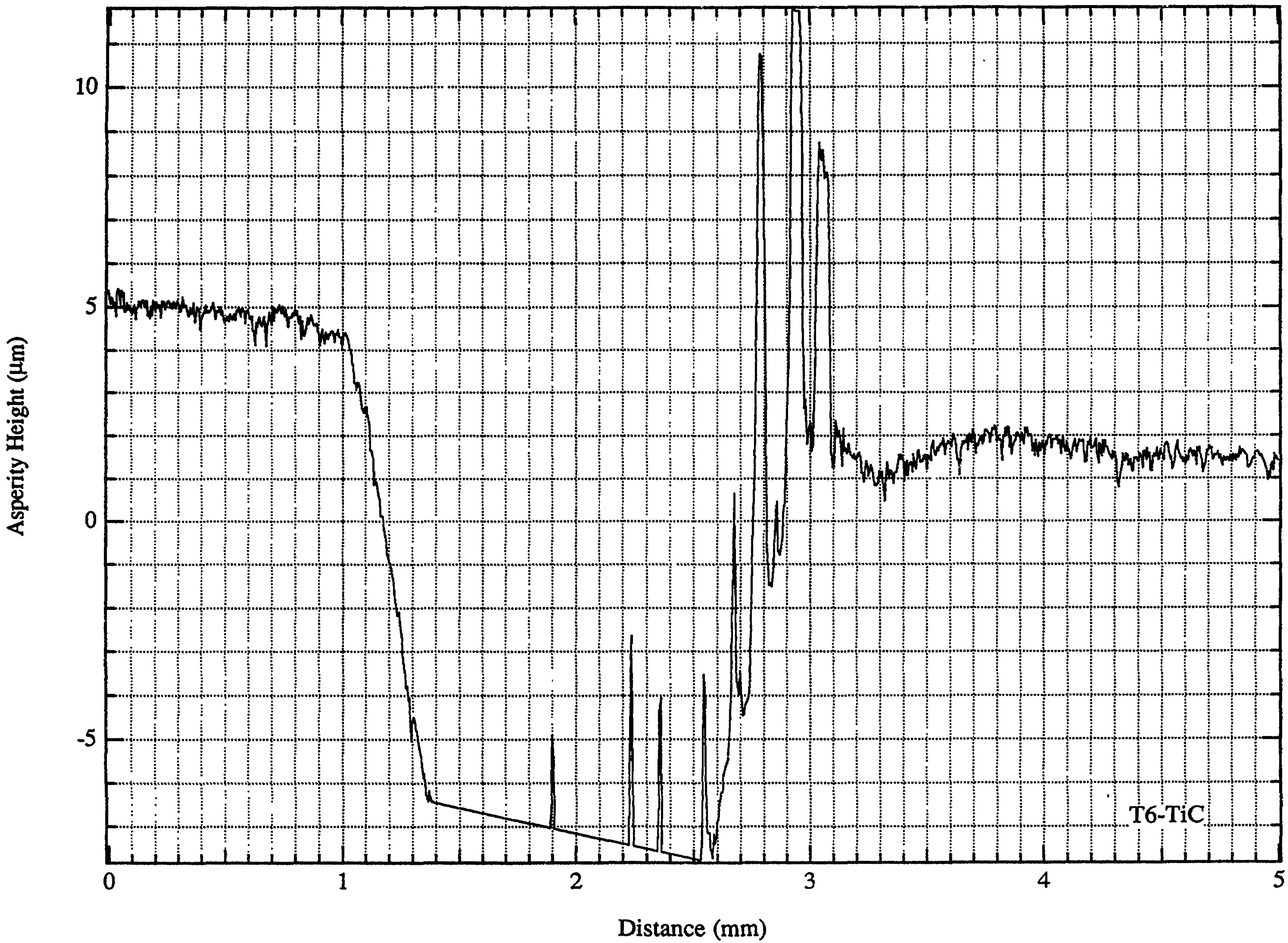

Asperity Height (µm)
10
5
0
-5
0
1
2
3
4
5
Distance (mm)
T6-TiC

PIN MATERIAL T
900°C

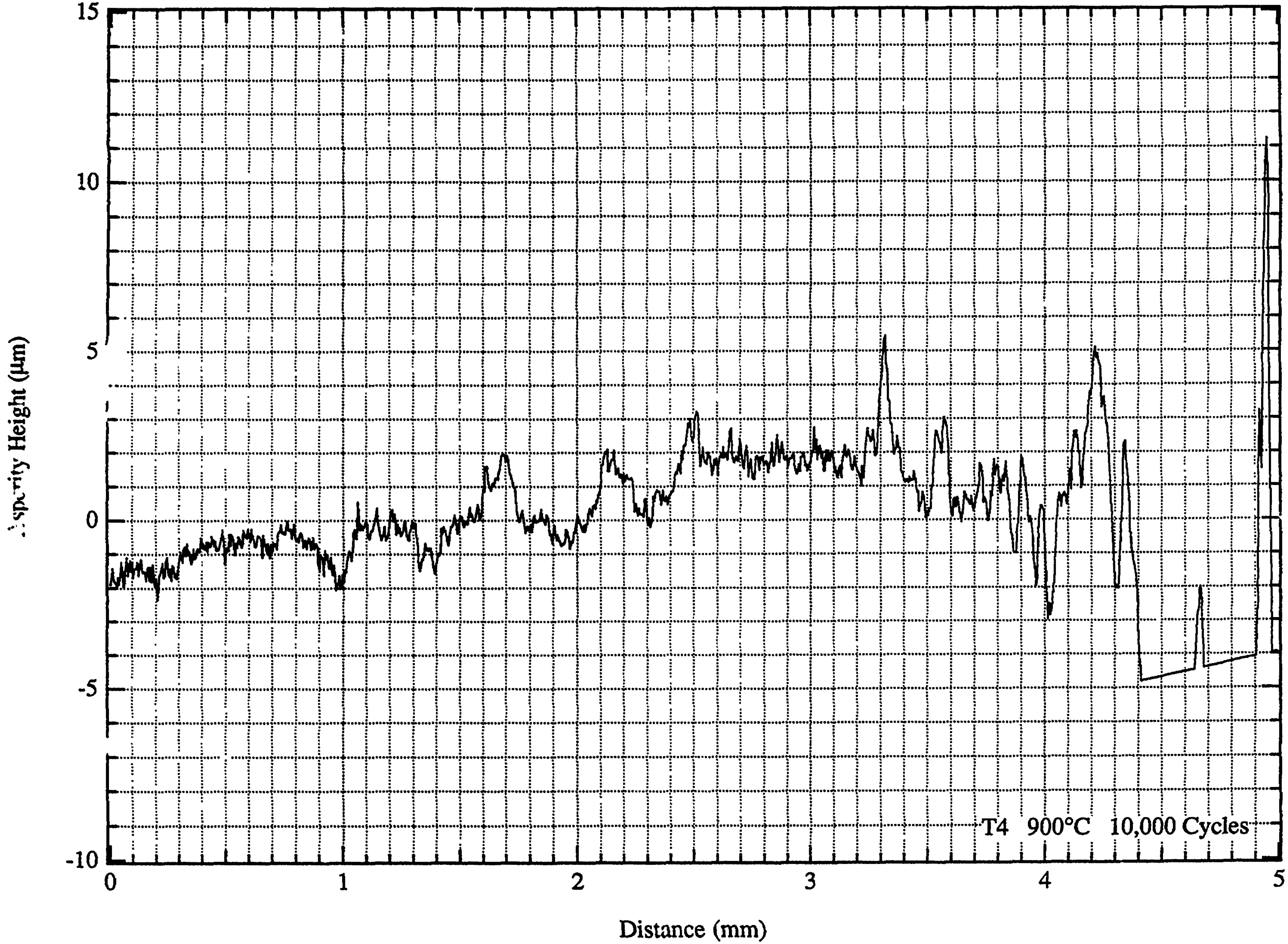
Asperity Height (µm)
15
10
5
0
-5
-10
0
1
2
3
4
5
Distance (mm)
T4 900°C 10,000 Cycles

52073 20X

Wear spot on pin.

52072 75X

Wear spot on pin.

52076 400X

Wear spot and debris.

52071 400X

Inside wear spot.

52075 1000X

Wear spot cracking.

52074 5000X

Absence of crack deflection by TiC particles, wear spot.

52083 30X

Wear track on flat.

52085 100X

Wear track on flat.

52086 2000X

Wear track damage (flat).

52088 12,000X

Wear track cracking (flat).

52087 8000X

Wear track and debris (flat).

Series II Southwest Research Institute WED 16-OCT-91 16:15
Cursor: 0 000KeV = 0 ROI (0) 4.300: 4.310

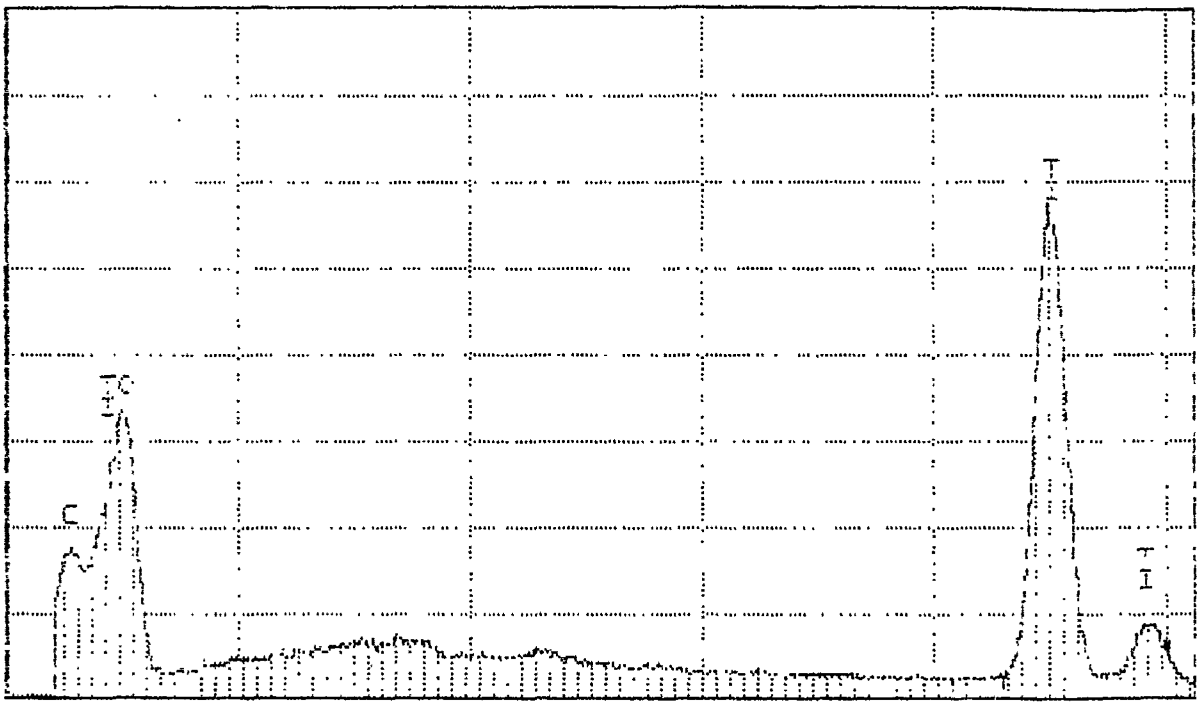

0 000 VFS = 4096 5 120
164 T4 WEAR PIN (DEBRIS 10KV UTW

Series II Southwest Research Institute WED 16-OCT-91 16:21
Cursor: 0.000KeV = 0 ROI (0) 4.300: 4.310

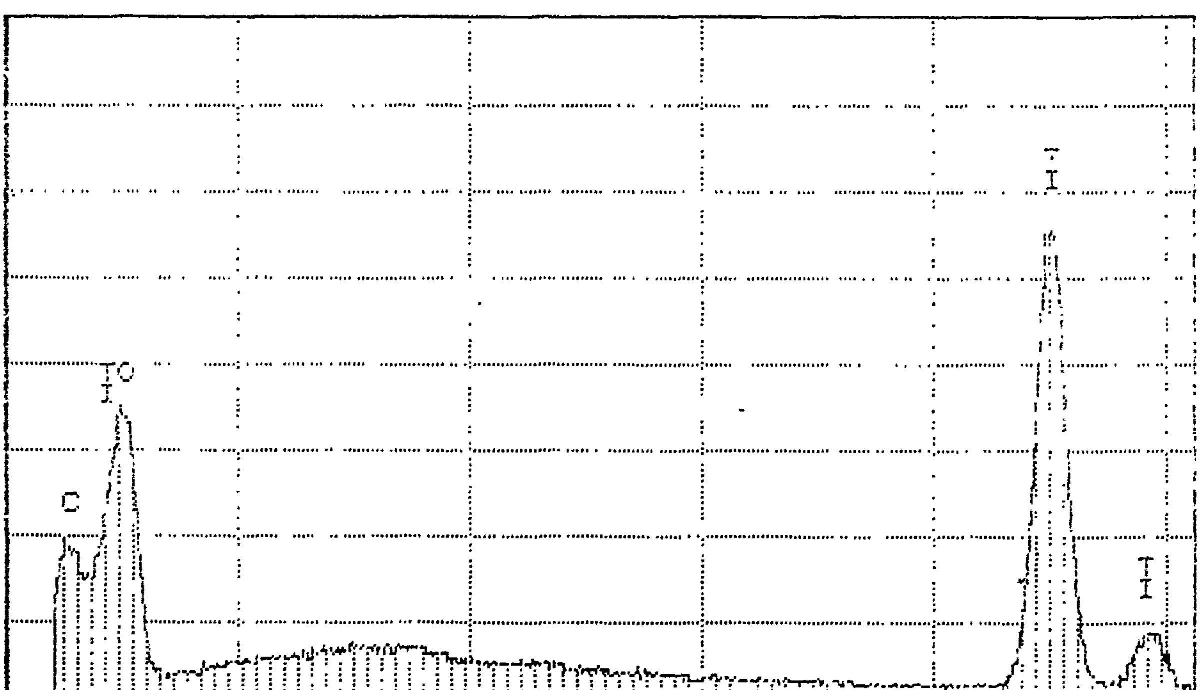

0.000 VFS = 4096 5.120
159 T4 WEAR PIN (INSIDE WEAR SPOT) 10KV UTW

Series II Southwest Research Institute THU 17-OCT-91 13:15
Cursor: 0.010keV = 0

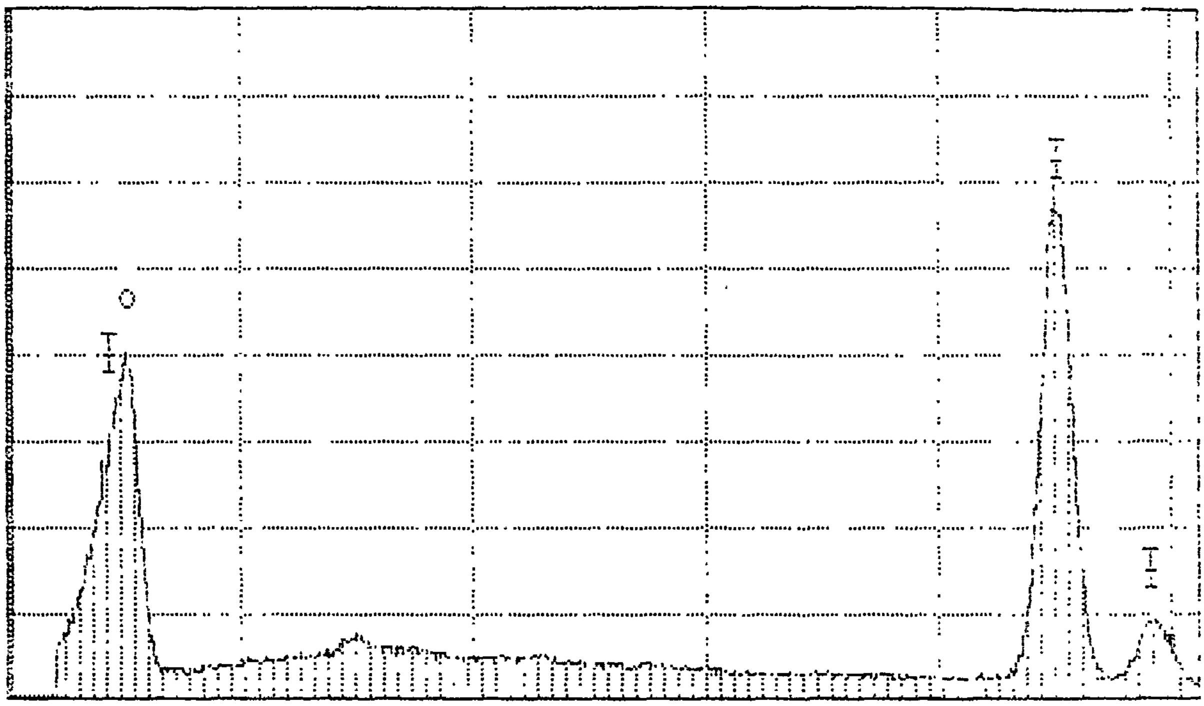

0.000 VFS = 4096 5.120
110 #5 TiC DEBRIS (WEAR TRACK) 10KV UTW

Series II Southwest Research Institute THU 17-OCT-91 13:19
Cursor: 0.010keV = 0

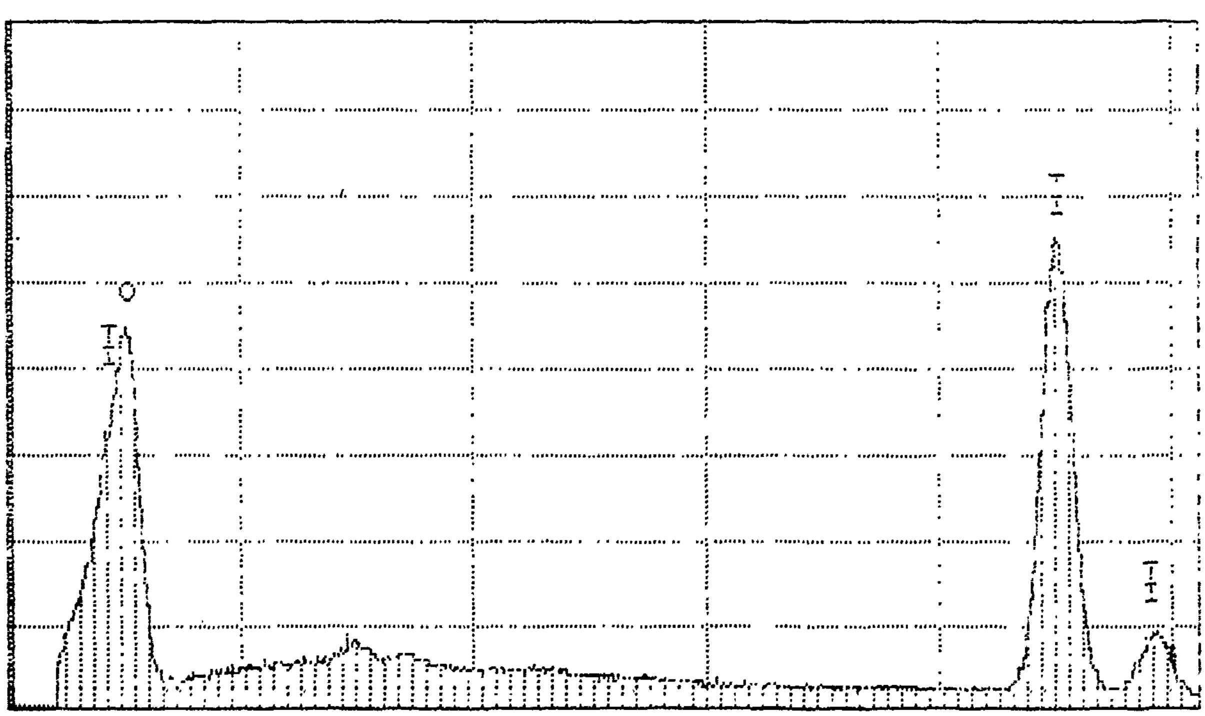

0.000 VFS = 4096 5.120
105 #5 TiC DEBRIS (INSIDE WEAR TRACK) 10KV UTW

Series II Southwest Research Institute THU 17-OCT-91 13:24

Cursor: 0.020keV = 0

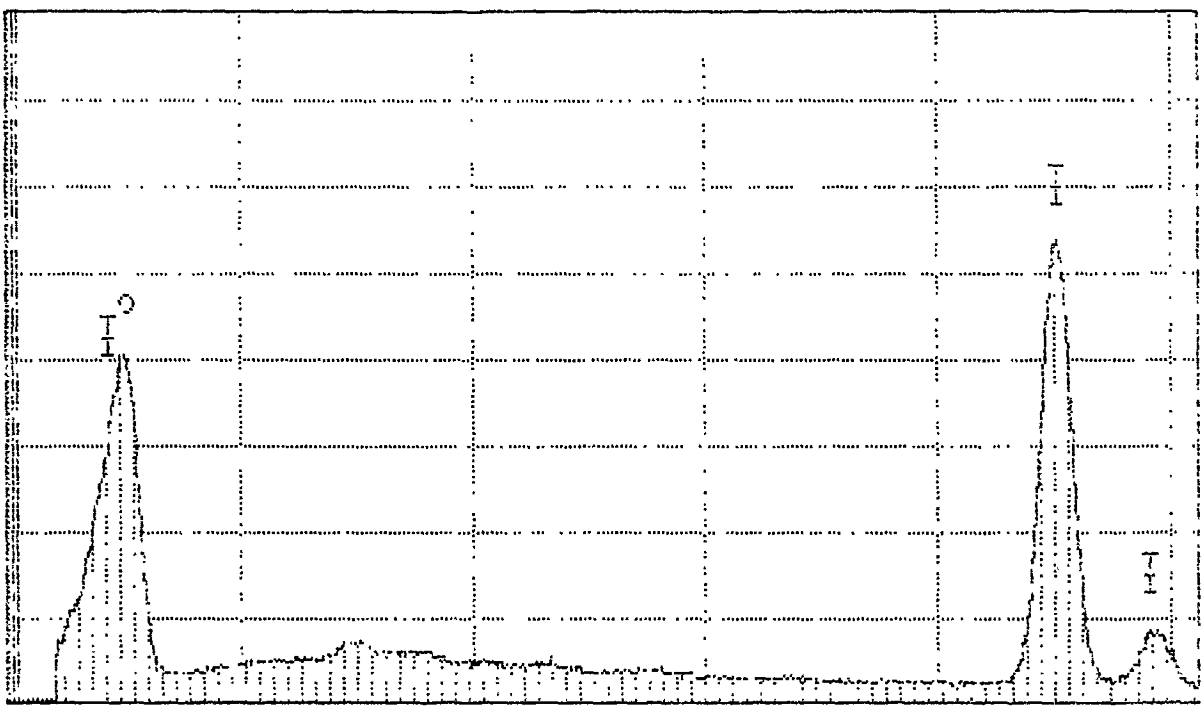

0.000 VFS = 4096 5.120

103 #5 TiC DEBRIS (OUTSIDE WEAR TRACK) 10KV UTW

PIN MATERIAL TC

23°C

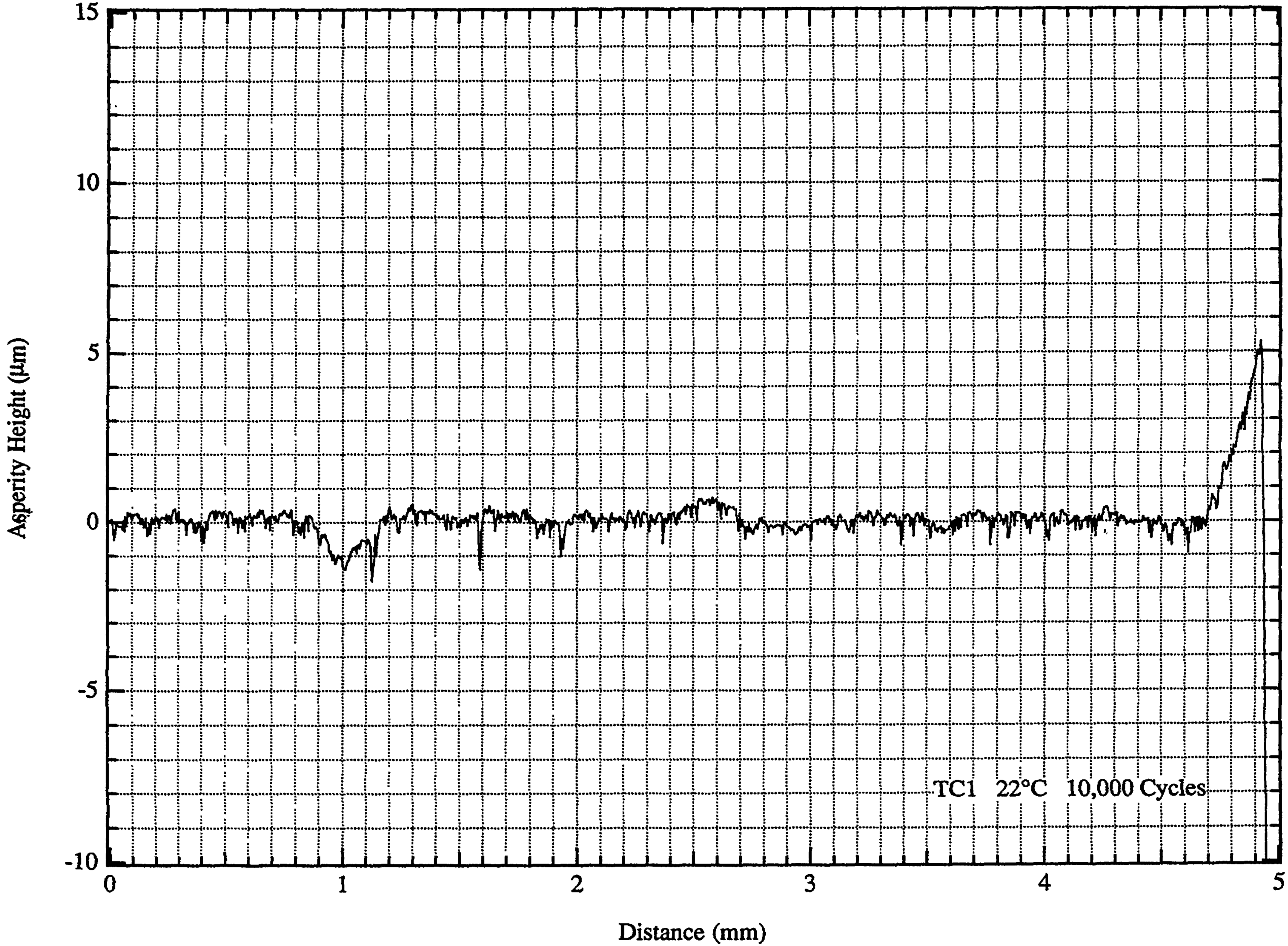
15
10
5
0
-5
-10
Asperity Height (µm)
0
1
2
3
4
5
Distance (mm)
TC1 22°C 10,000 Cycles

TC

Spec. No.	σ_μ(MPa)	σ_{AE} (Mpa)
1	1642	1174
2	1821	1159
3	1916	1191

PIN MATERIAL TC
600°C

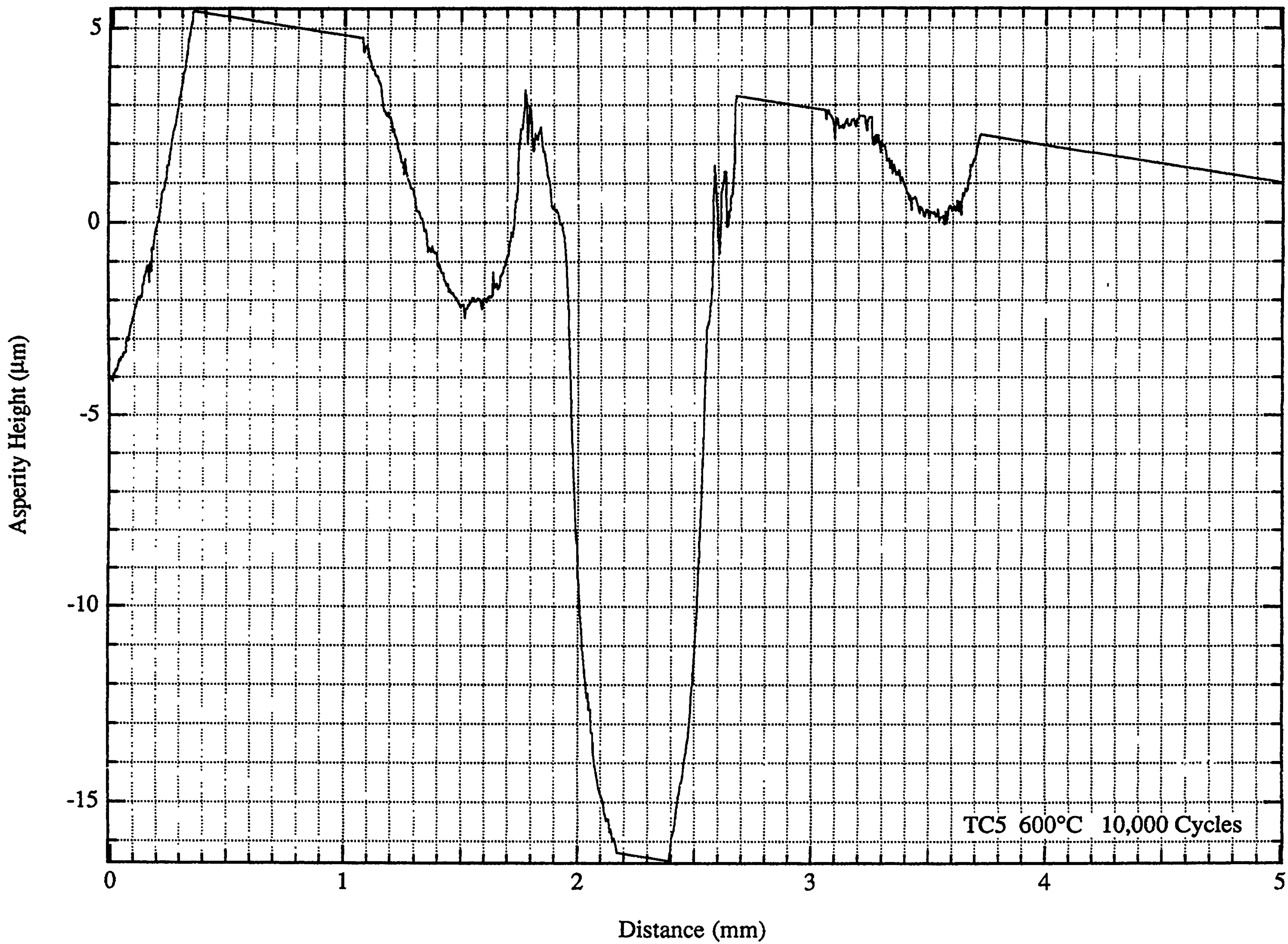

Asperity Height (μm)
5
0
-5
-10
-15
0
1
2
3
4
5
Distance (mm)
TC5 600°C 10,000 Cycles

PIN MATERIAL TC
900°C

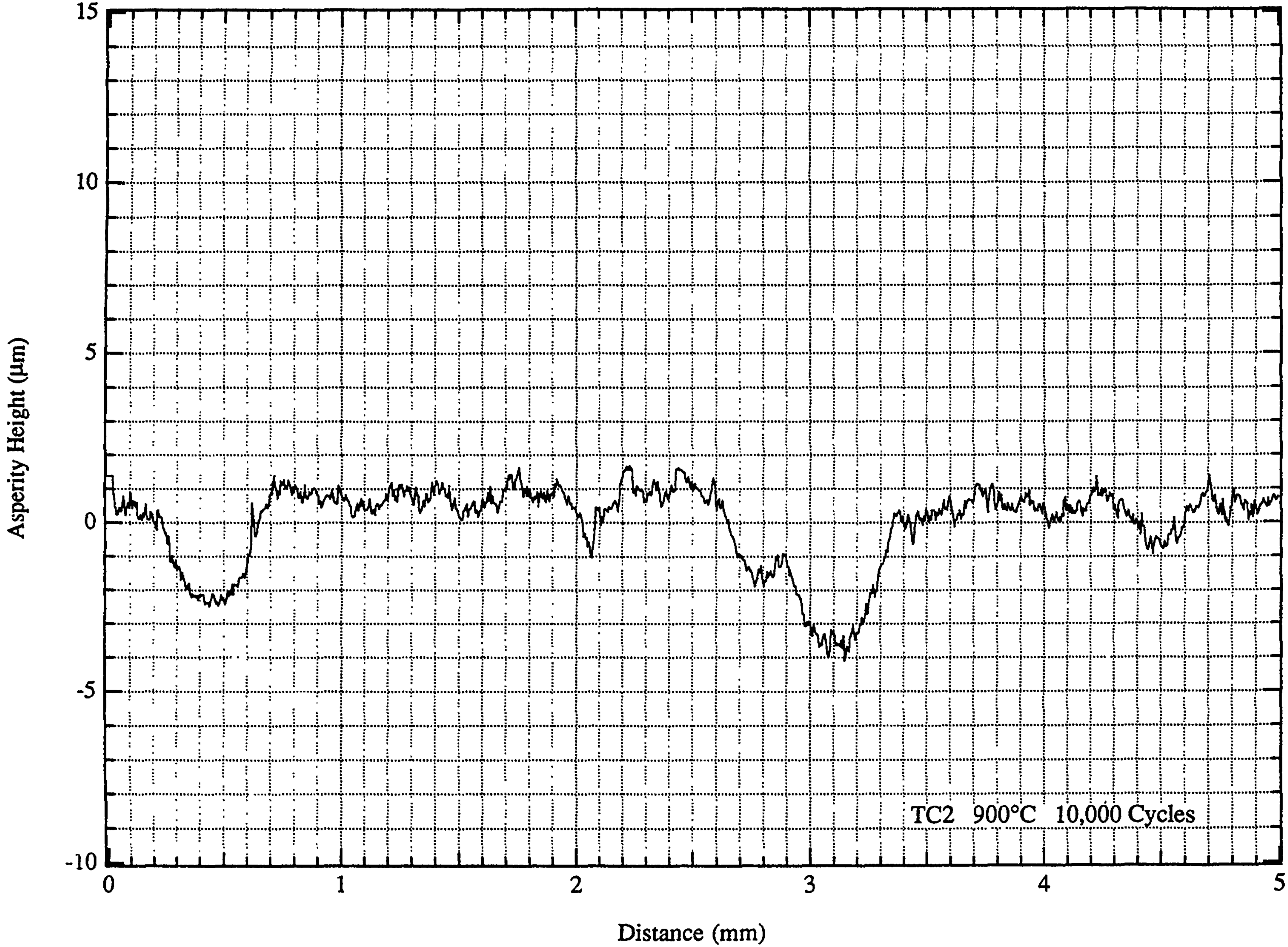
15
10
5
0
-5
-10
0
1
2
3
4
5
Asperity Height (µm)
Distance (mm)
TC2 900°C 10,000 Cycles

PIN MATERIAL TVC
23°C

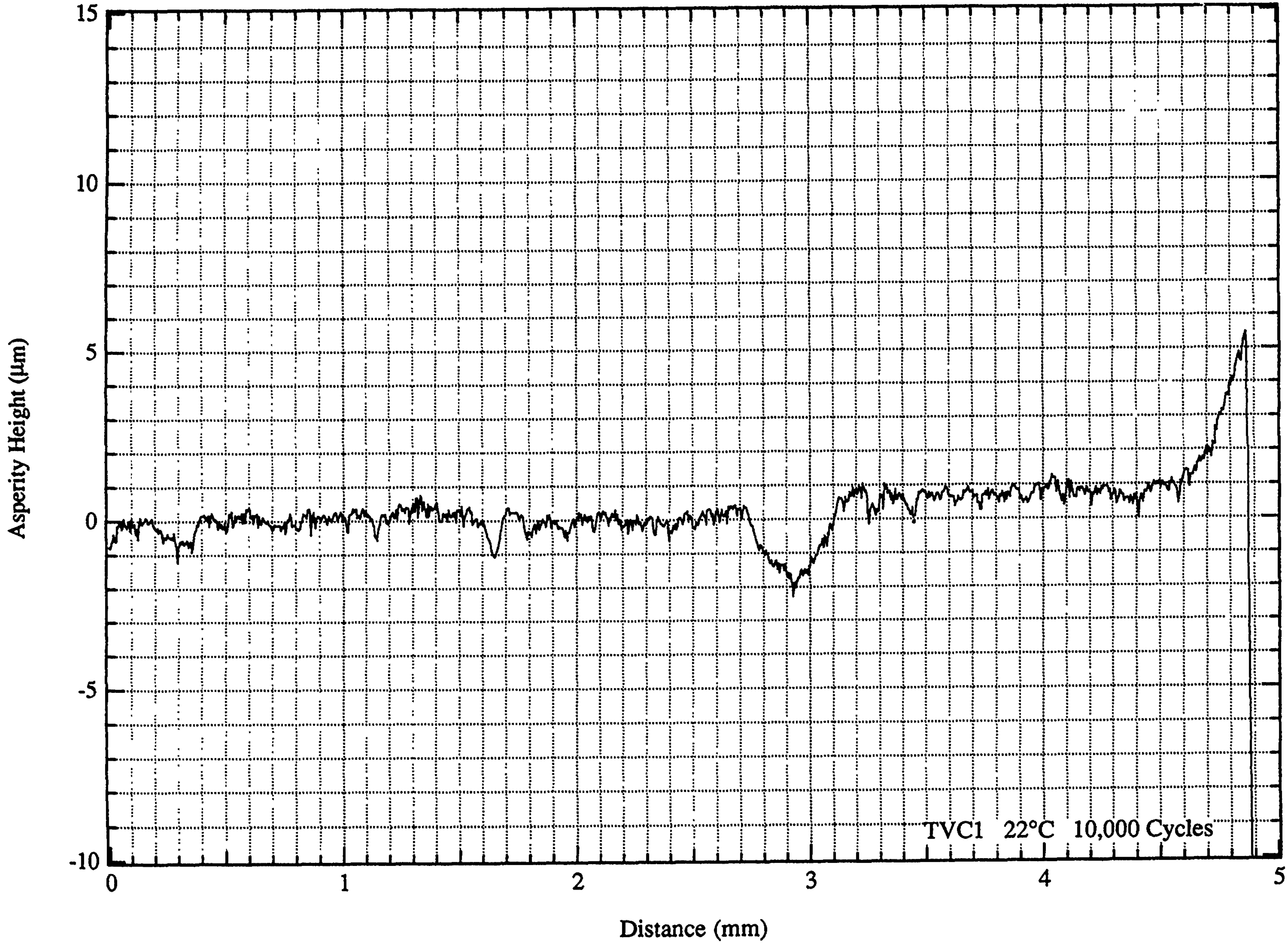
Asperity Height (µm)
15
10
5
0
-5
-10
0
1
2
3
4
5
Distance (mm)
TVC1 22°C 10,000 Cycles

TVC

Spec. No.	σ_{μ}(MPa)	σ_{AE} (Mpa)
1	1086	902
2	742	614
3	1309	860

PIN MATERIAL TVC
600°C

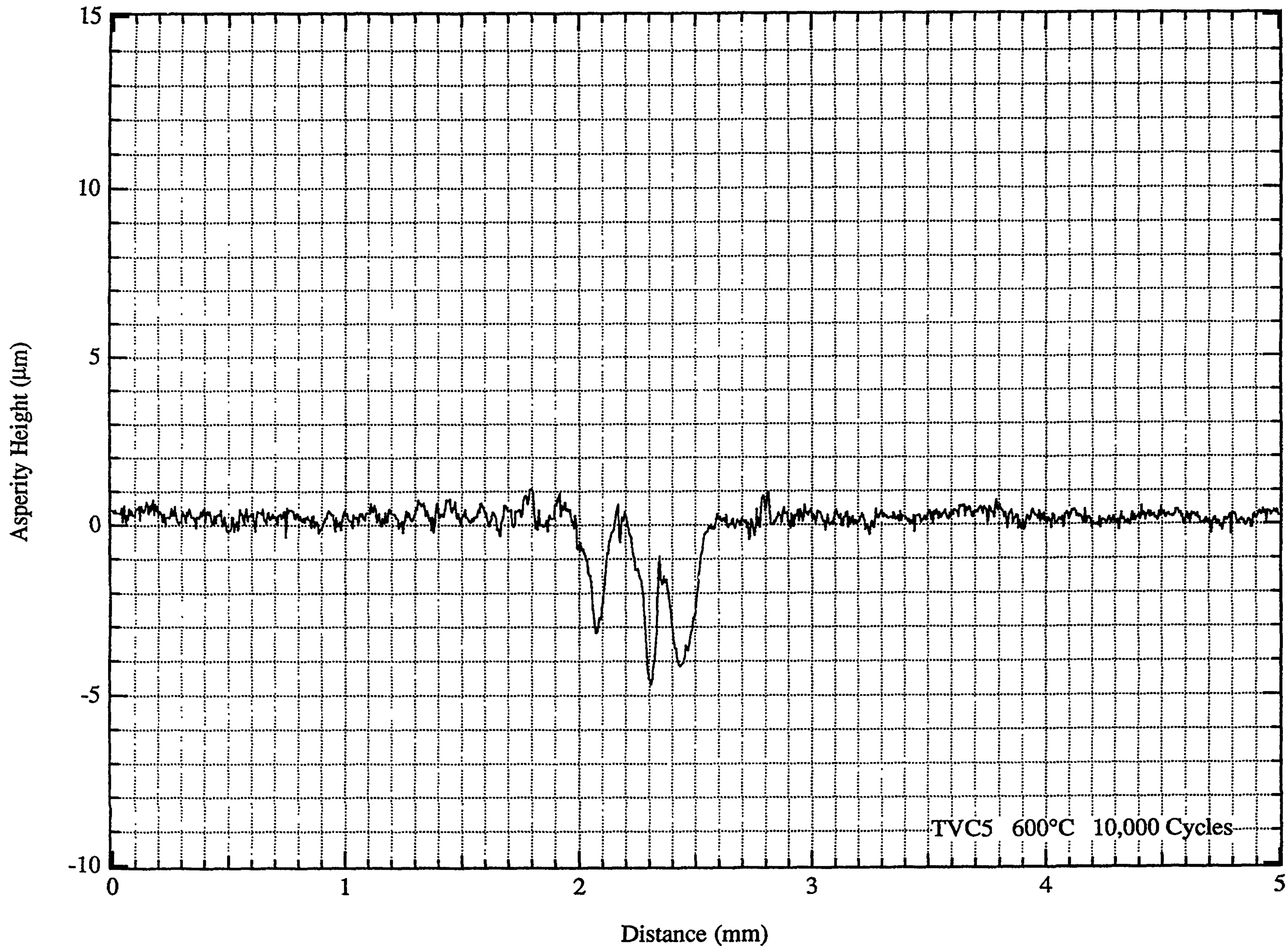
15
10
5
0
-5
-10
Asperity Height (µm)
0
1
2
3
4
5
Distance (mm)
TVC5 600°C 10,000 Cycles

52090 20X
Wear spot on pin.

52091 100X
Wear spot on pin.

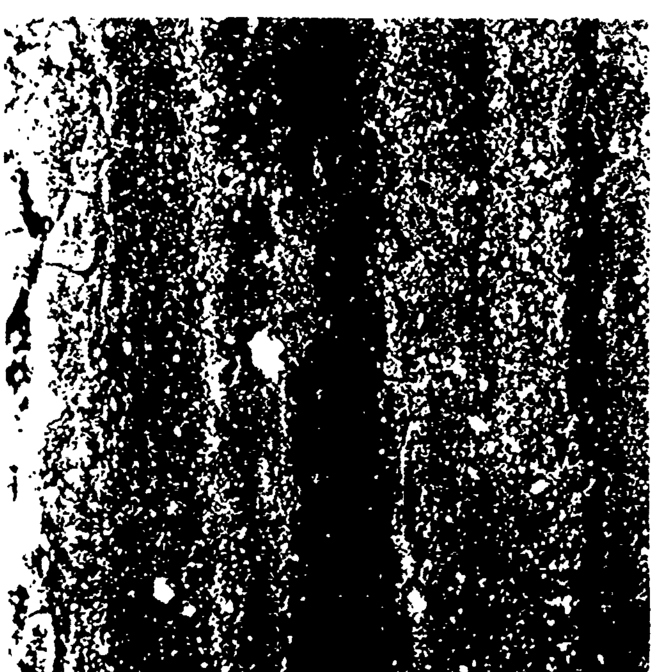

52092 1000X
Oxide cracking within wear spot (pin).

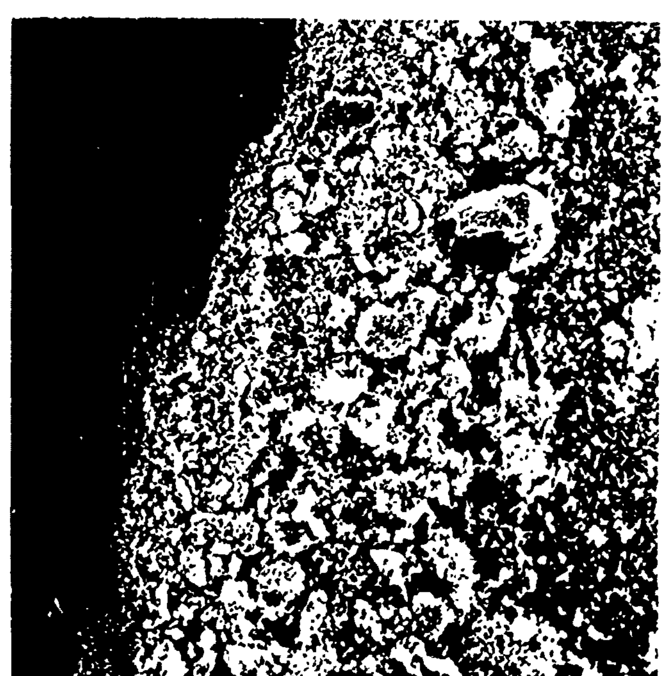

52095 400X
Interface between wear spot (pin and debris.

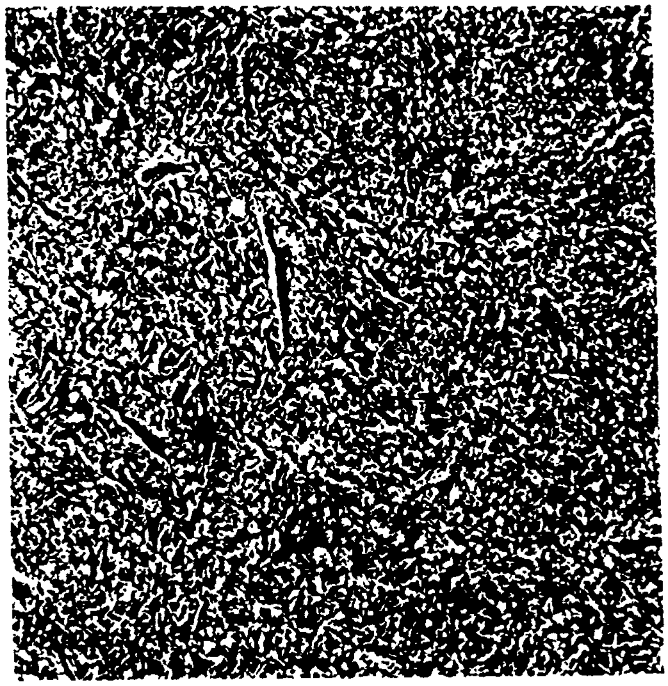

52093 500X

Outside wear spot (pin).

52094 5000X

Outside wear spot (pin).

52096 30X
Wear track on flat.

52097 100X
Wear track on flat.

52099 600X
Inside wear track.

52098 1000X
Inside wear track.

* ' ·

Series II Southwest Research Institute FRI 18-OCT-91 10:39
Cursor: 0.000KeV = 0

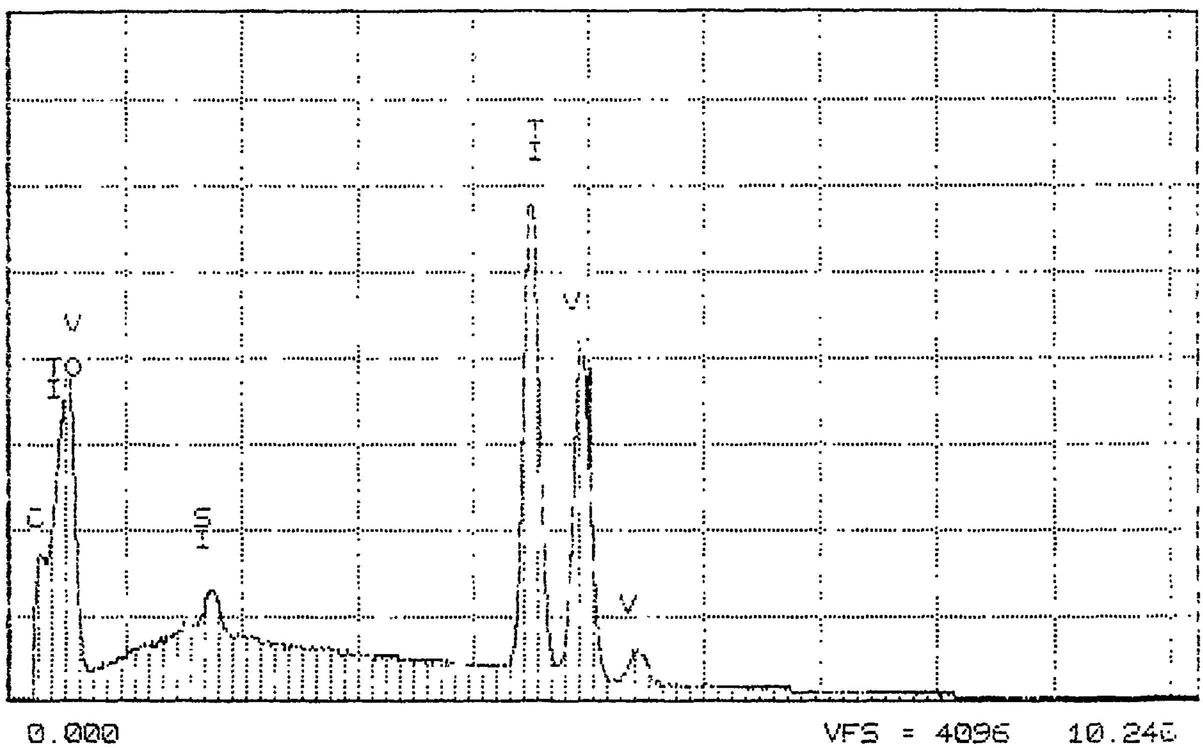

233 TVC5 PIN (DEBRIS) ADJ WEAR SPOT 10KV UTW

0,0
*

Series II Southwest Research Institute FRI 18-OCT-91 10:46
Cursor: 0.000KeV = 0

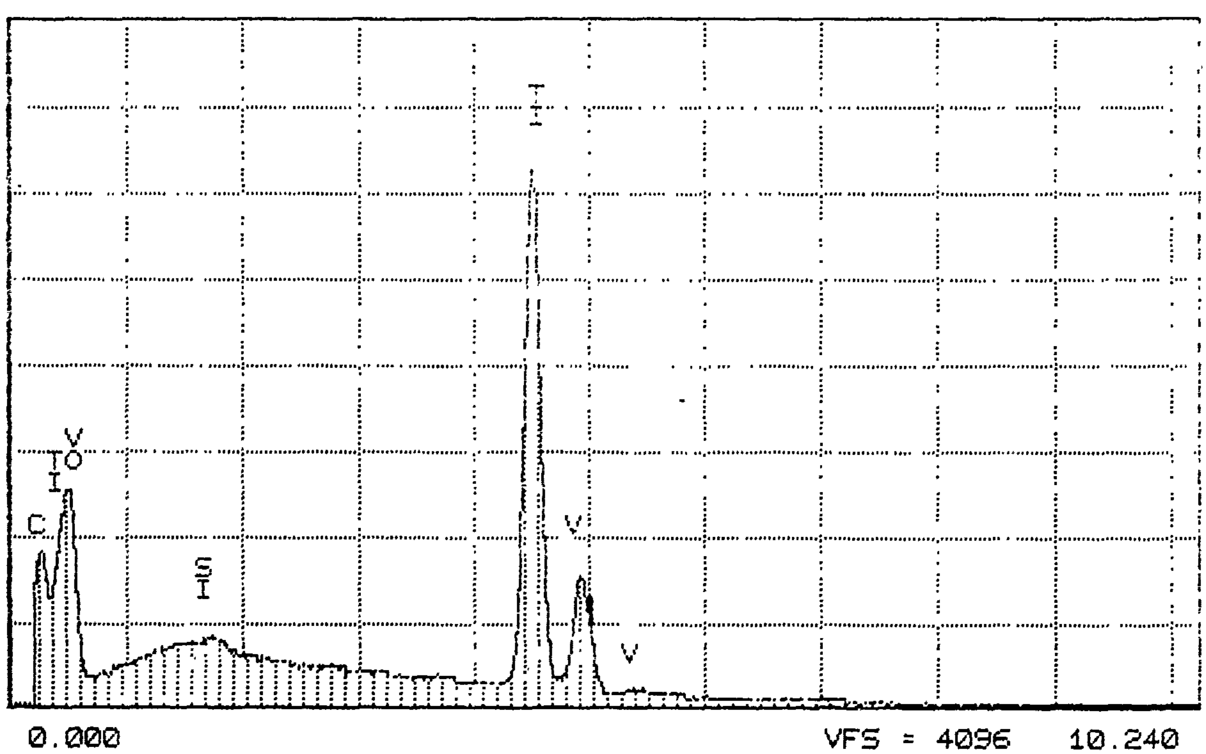

160 TVC5 PIN (WEAR SPOT) 10KV UTW

SQ: QUANTIFY

TVC5 PIN (AWAY FROM WEAR SPOT) 20KV WD19
Standardless Analysis
20.0 KV 36.3 Degrees

Chi-sqd = 2.22

Element	Rel. K-ratio	Net Counts
Ti-K	0.55644 +/- 0.00364	103781 +/- 679
V -K	0.43992 +/- 0.00352	73120 +/- 585
Si-K	0.00363 +/- 0.00060	978 +/- 161

ZAF Correction 20.00 KV 36.30 deg
No.of Iterations = 1

Element	K-ratio	Z	A	F	Atom%	Wt%
Ti-K	0.555	0.992	1.004	1.000	56.53	55.25
V -K	0.438	1.012	0.997	1.000	42.55	44.22
Si-K	0.004	0.892	1.652	0.996	0.93	0.53
					Total=	100.00%

Series II Southwest Research Institute FRI 12-OCT-91 10:31
Cursor: 0.000keV = 0

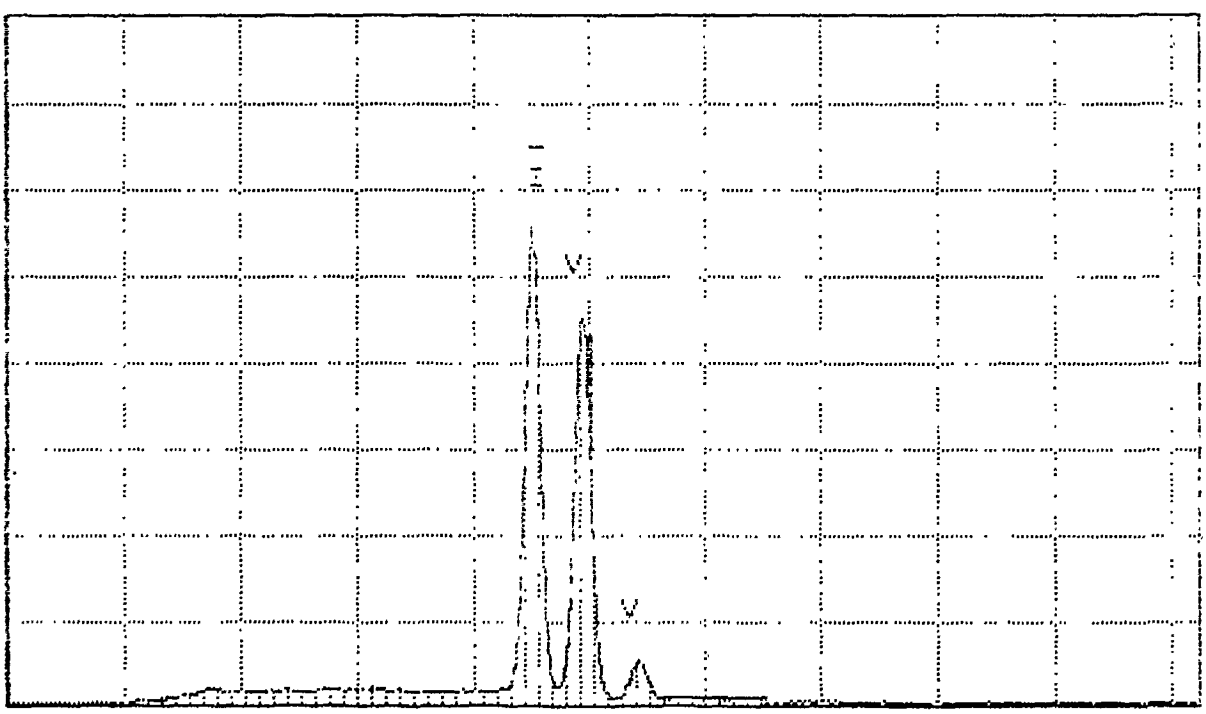

0.000 VFS = 8192 10.240
252 TVC5 PIN (AWAY FROM WEAR SPOT) 20KV WD19

1,30

*

Series II Southwest Research Institute   FRI 18-OCT-91 12:58
Cursor: 0.000KeV = 0

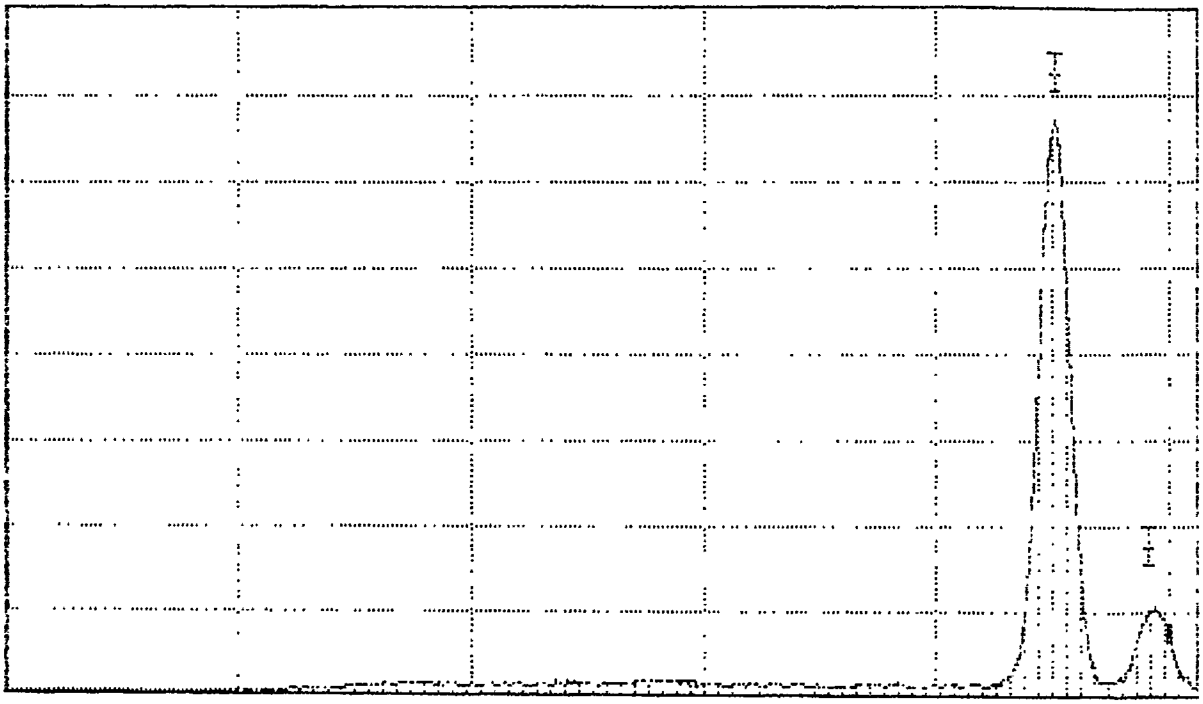

0.000   VFS = 4096   5.120
86   #14 FLAT TVC (DEBRIS) 20KV WD=20

0,0

Series II Southwest Research Institute   FRI 18-OCT-91 13:04
Cursor: 0.000KeV = 0

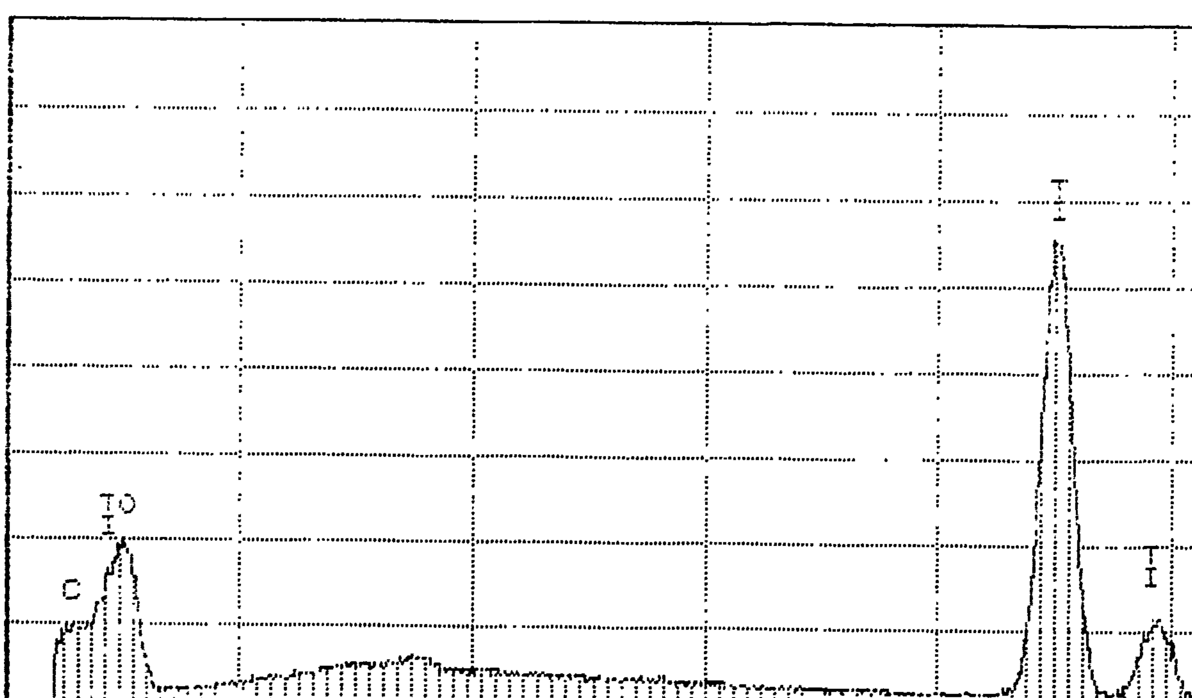

0.000   VFS = 4096   5.120
139   #14 FLAT TVC   (DEBRIS)   10KV UTW

Series II Southwest Research Institute FRI 18-OCT-91 13:18

Cursor: 0 000KeV = 0

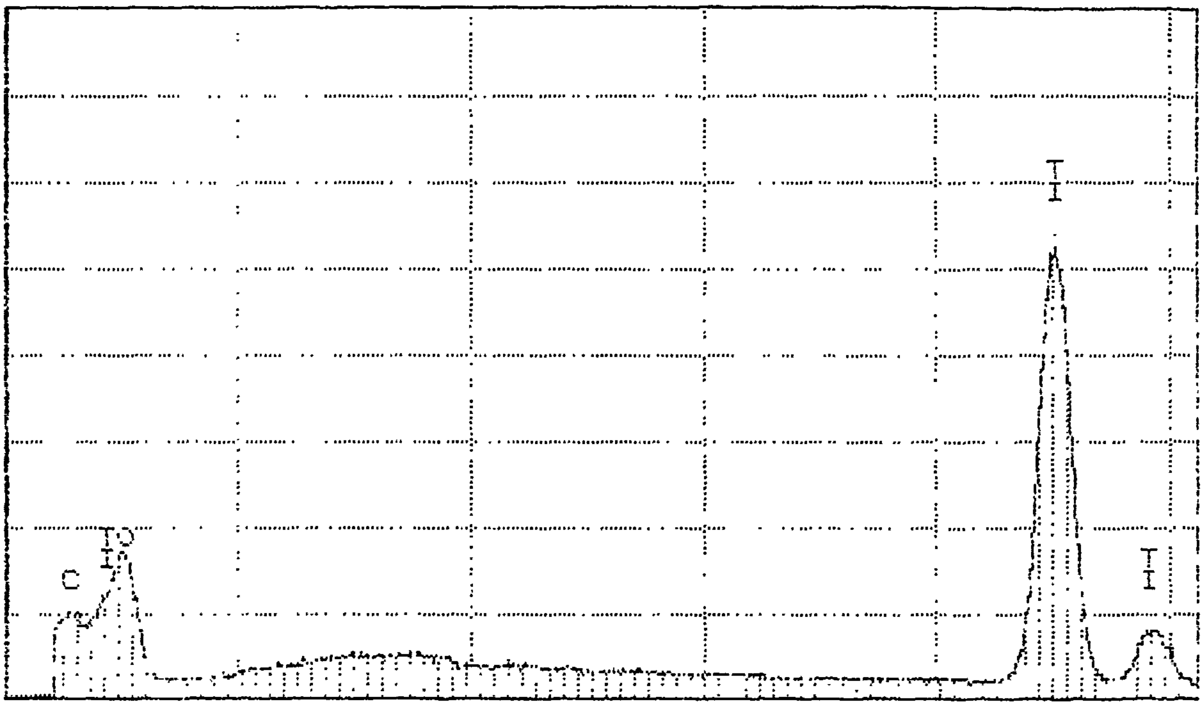

0.000 VFS = 4095 5.120

105 #14 FLAT TVC (DEBRIS IN WEAR TRACK) 10KV UTW

PIN MATERIAL TBC
23°C

TBC

Spec. No.	σ_{μ}(MPa)	σ_{AE} (Mpa)
1	822	610
2	897	700
3	1013	859

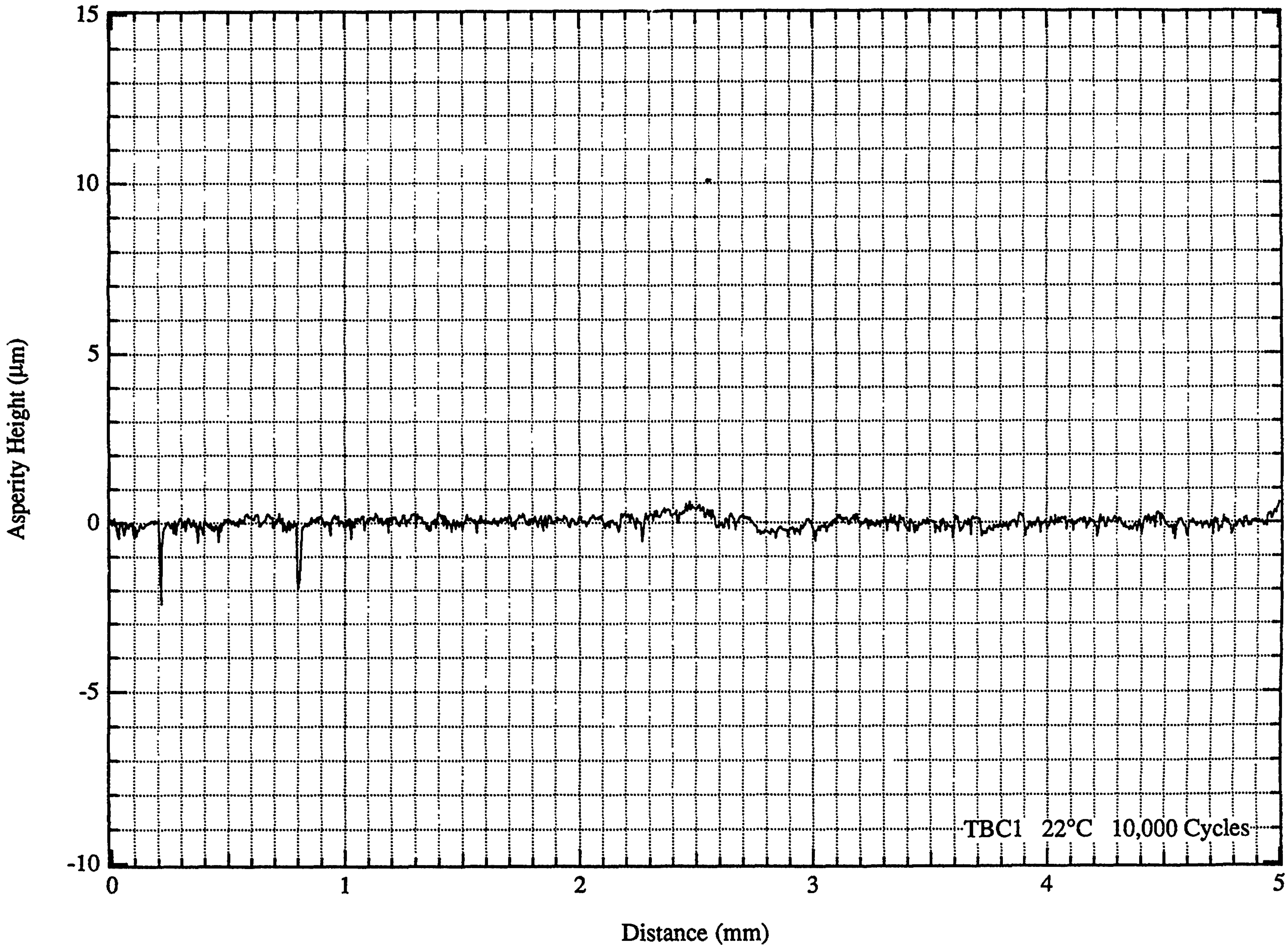
Asperity Height (µm)
15
10
5
0
-5
-10
0
1
2
3
4
5
Distance (mm)
TBC1 22°C 10,000 Cycles

51891 75X

Wear spot on pin.

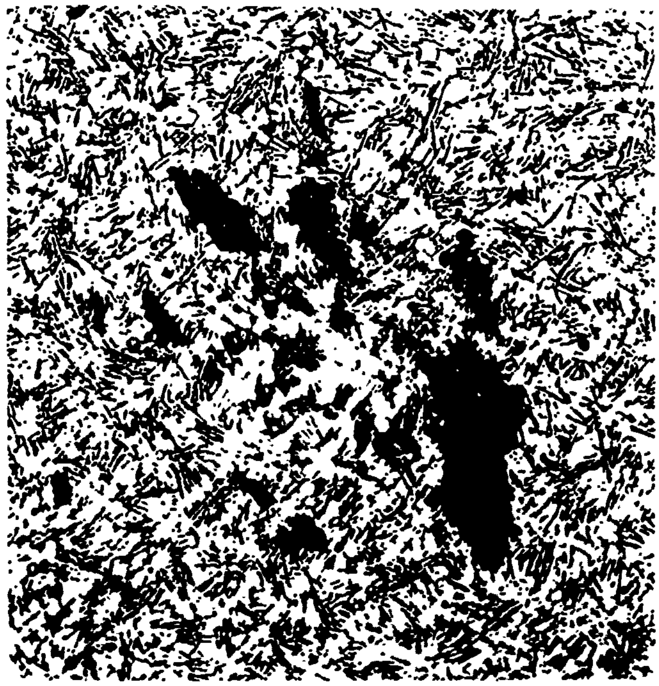

51890 75X

Backscattered electron image of wear spot on pin, showing oxide debris (dark regions); graphite (fine scale particles); and TiC matrix (light).

51892 400X

Wear spot and debris.

51893 400X

Backscattered electron image of wear spot and debris.

Series II Southwest Research Institute THU 03-OCT-91 13:08
Cursor: 0.000KeV = 0

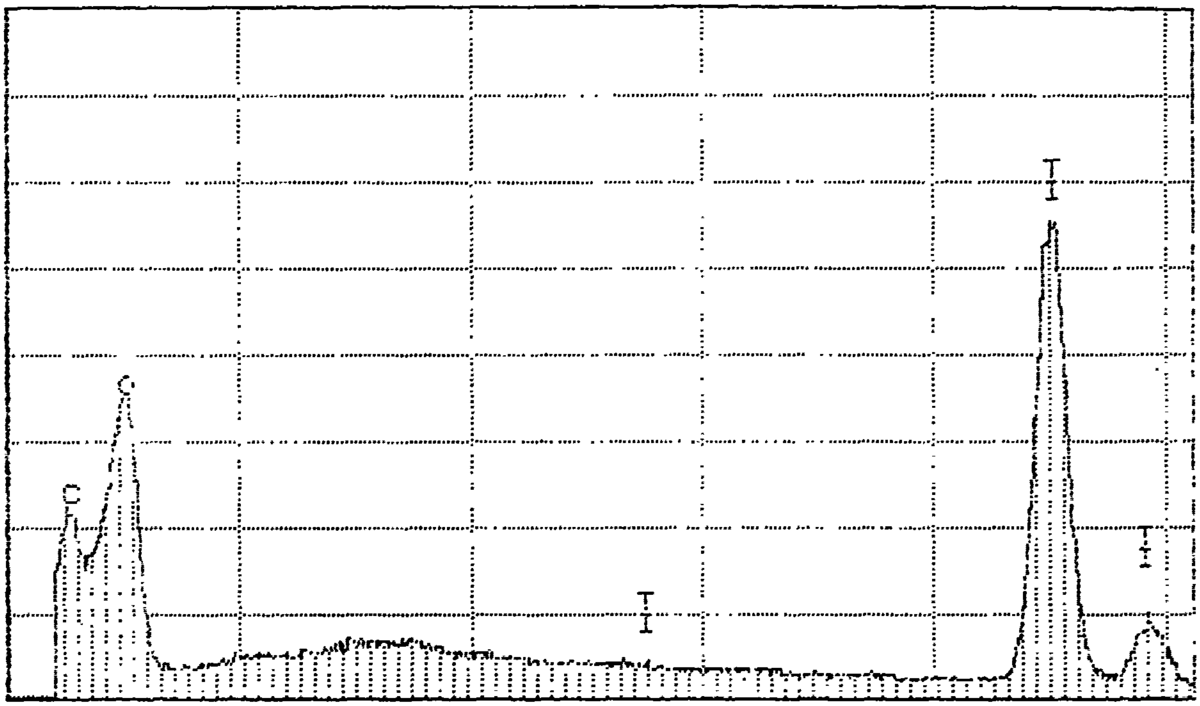

0.000 VFS = 4096 5.120
140 TIBC-1 WEAR SPOT DEBRIS (UTW) 10KV

Series II Southwest Research Institute THU 03-OCT-91 13:15
Cursor: 0.000KeV = 0

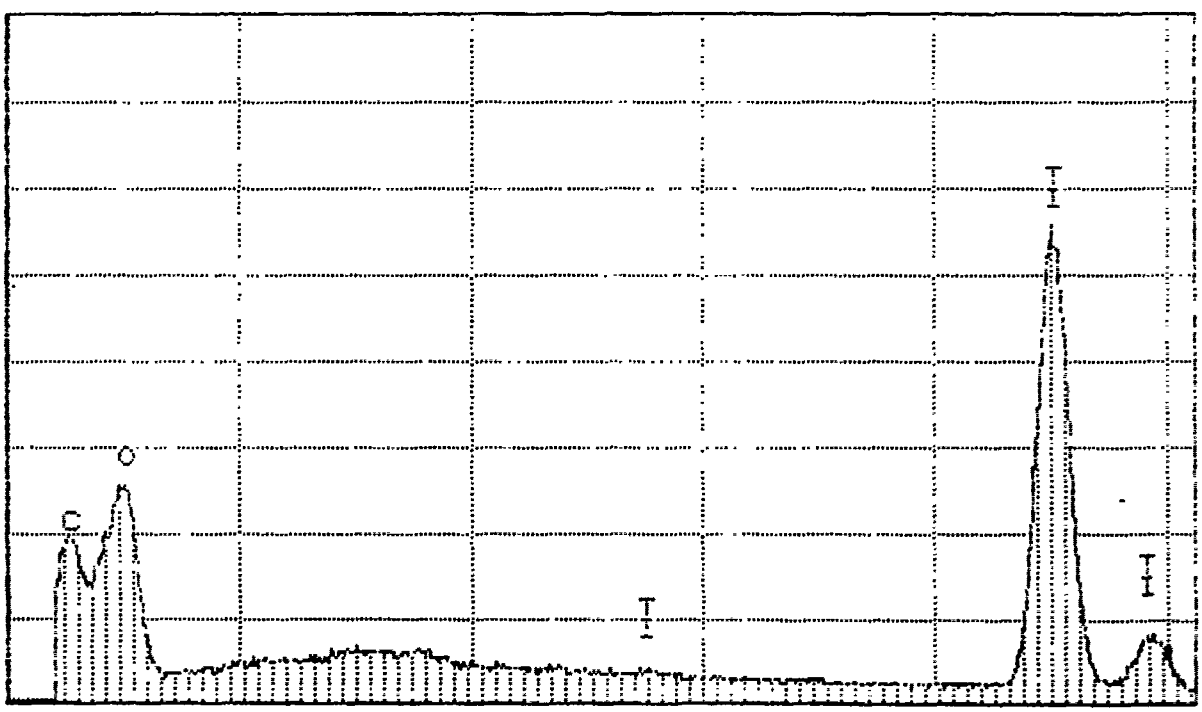

0.000 VFS = 4096 5.120
107 TIBC-1 INSIDE WEAR SPOT (UTW) 10KV

Series II Southwest Research Institute THU 03-OCT-91 13:20

Cursor: 0.000KeV = 0

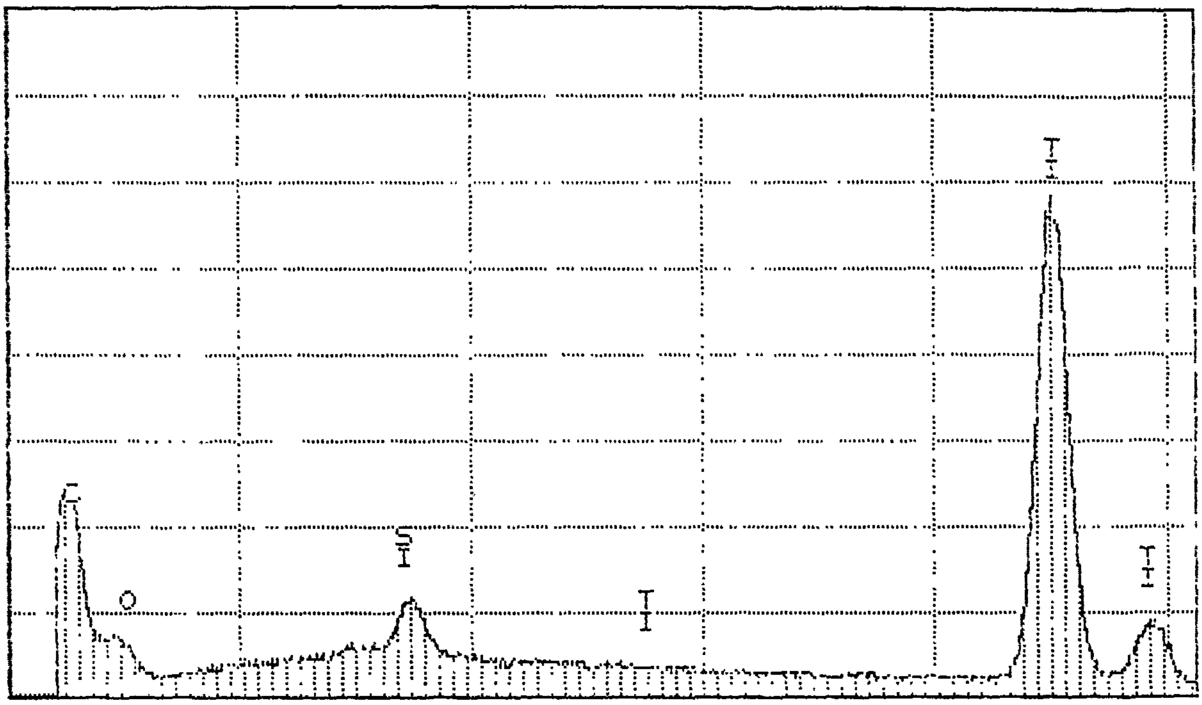

0.000 VFS = 4096 5.120

115 TIBC-1 OUTSIDE WEAR SPOT (JTW) 10KV

PIN MATERIAL TBC
600°C

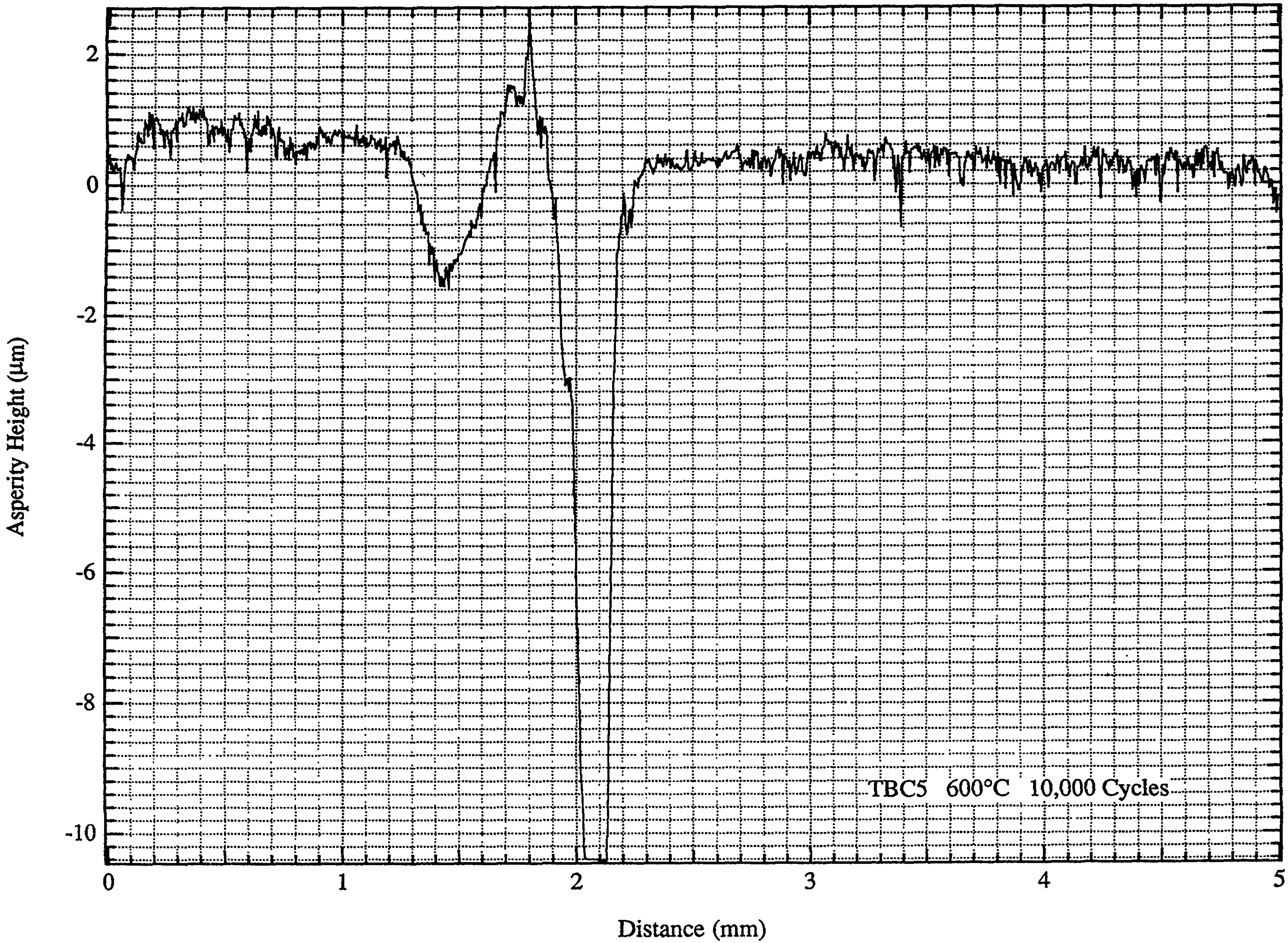
Asperity Height (µm)
2
0
-2
-4
-6
-8
-10
0
1
2
3
4
5
Distance (mm)
TBC5 600°C 10,000 Cycles

PIN MATERIAL TBC
900°C

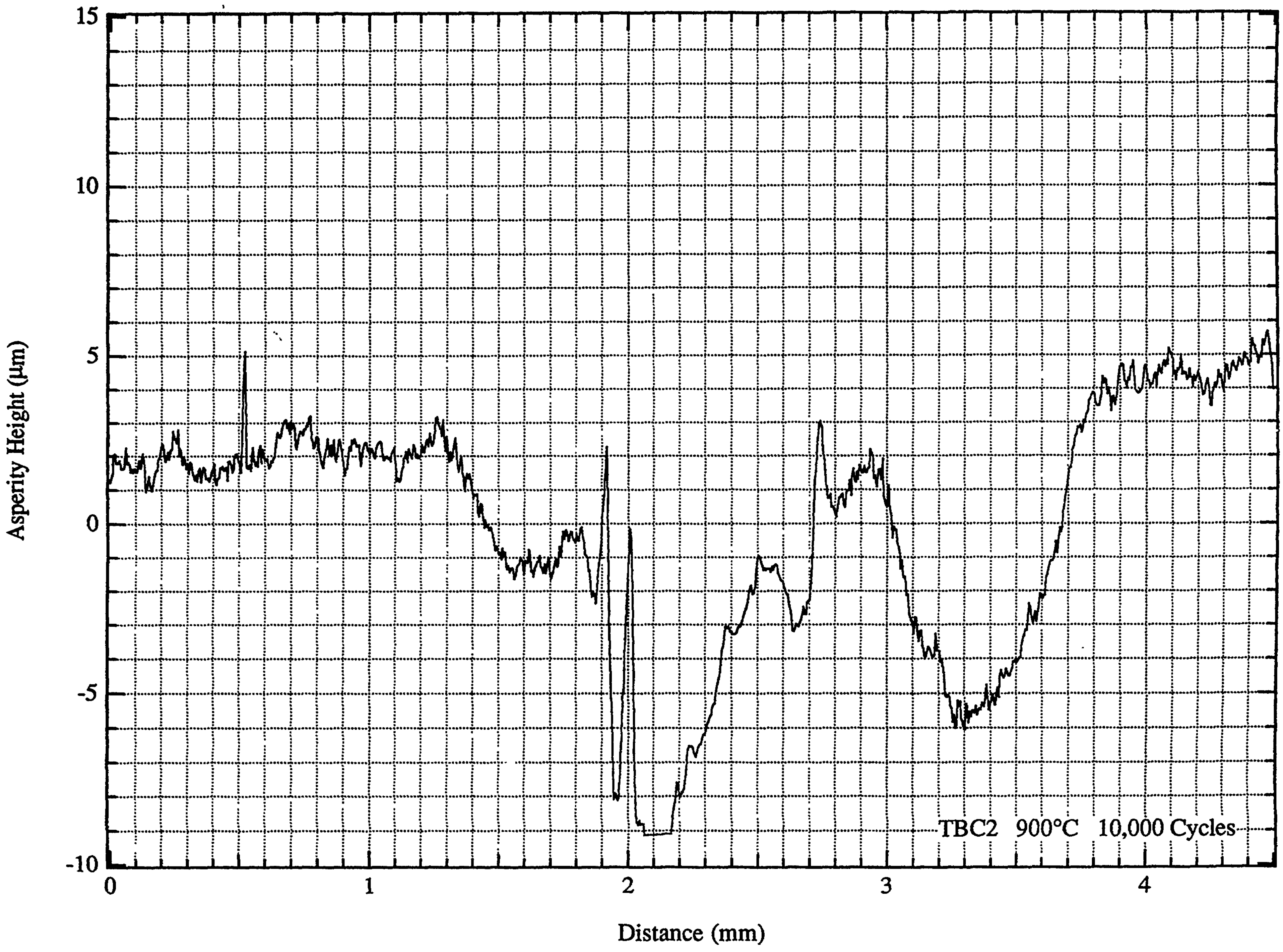

15
10
5
0
-5
-10
Asperity Height (µm)
0
1
2
3
4
Distance (mm)
TBC2 900°C 10,000 Cycles

51902 30X

Wear track on flat.

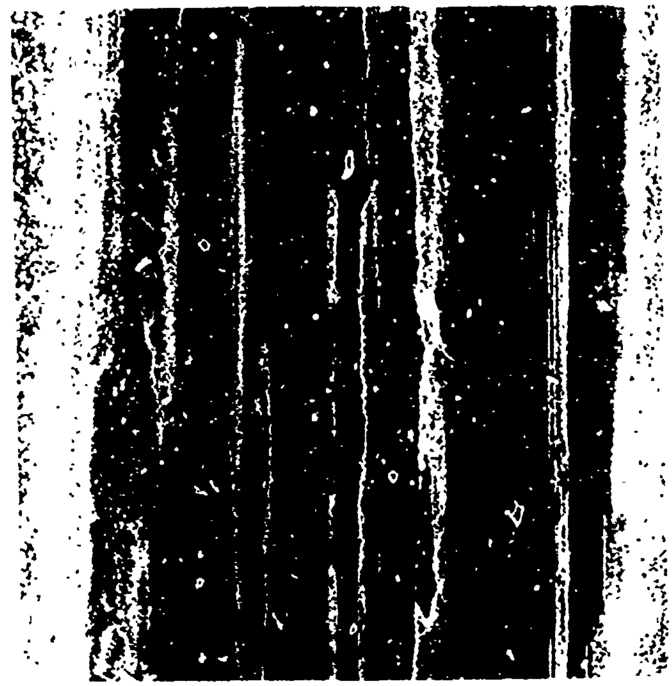

51903 80X

Middle of wear track.

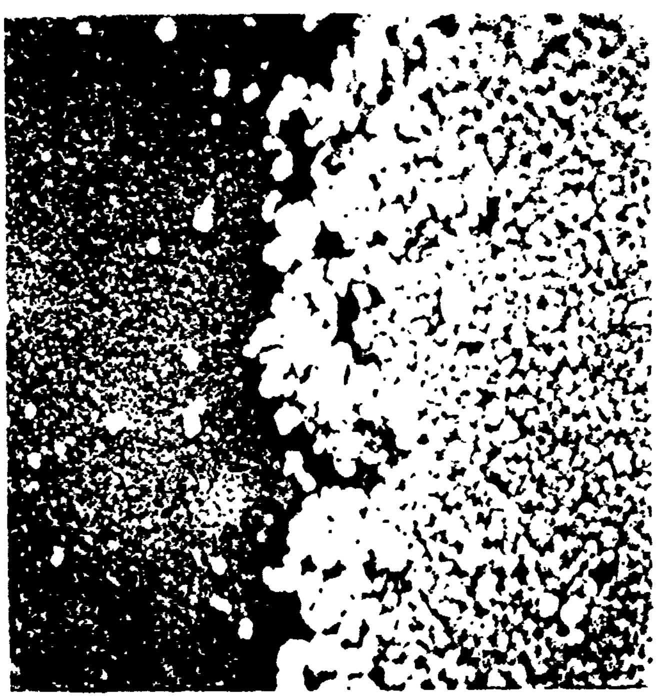

51905 5000X

Debris inside wear track.

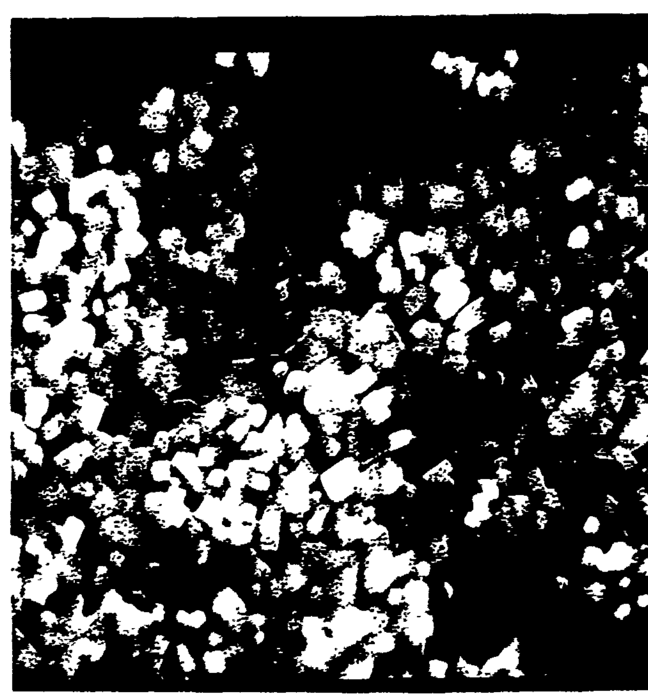

51906 8000X

Wear track.

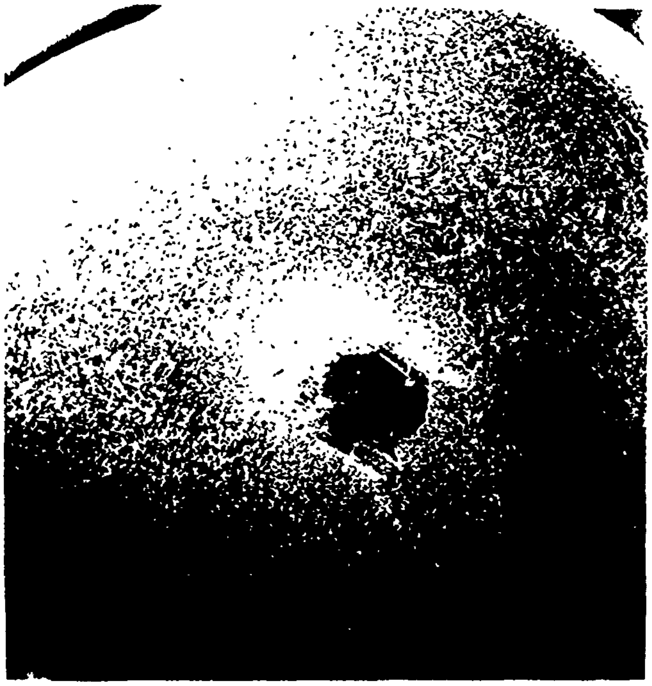

51897 20X

Wear spot on pin.

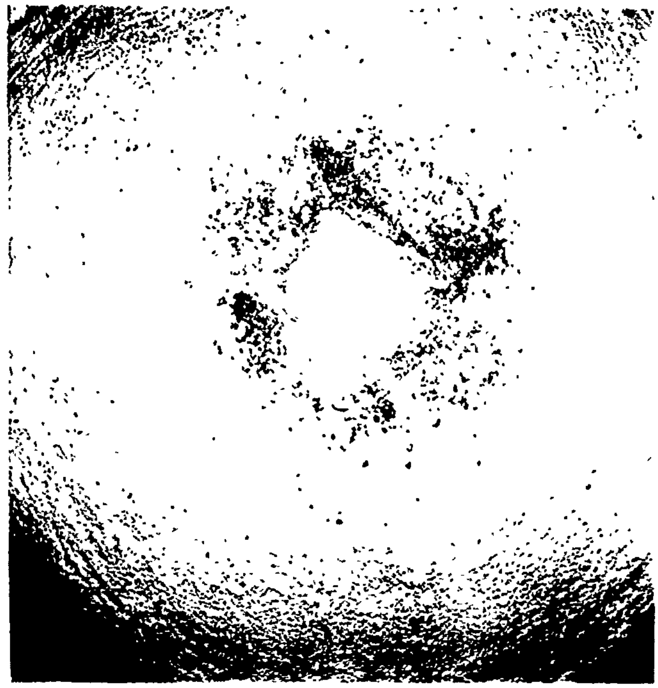

51898 20X

Backscatter electron image of wear spot on pin.

51901 400X

Interface between wear spot and debris.

Series II Southwest Research Institute THU 03-OCT-91 14:13
Cursor: 0.000keV = 0

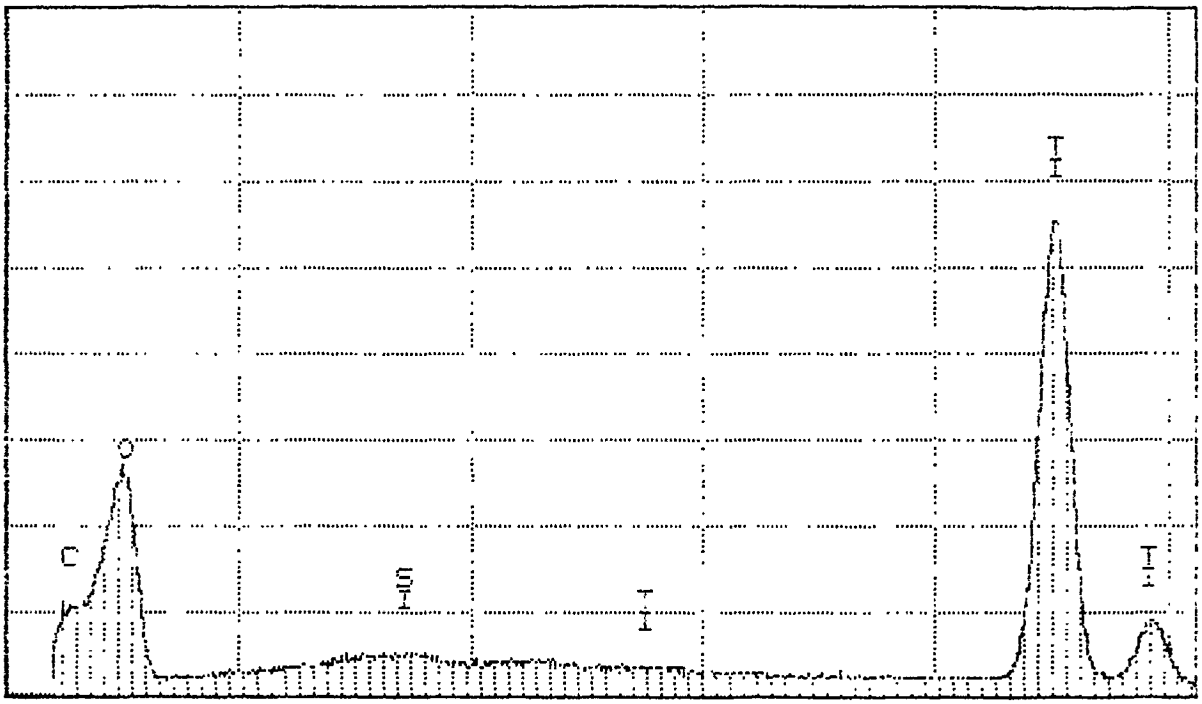

0.000 VFS = 4096 5.120
115 TIBC-2 WEAR SPOT DEBRIS (UTW) 10KV

Series II Southwest Research Institute THU 03-OCT-91 14:19
Cursor: 0.000keV = 0

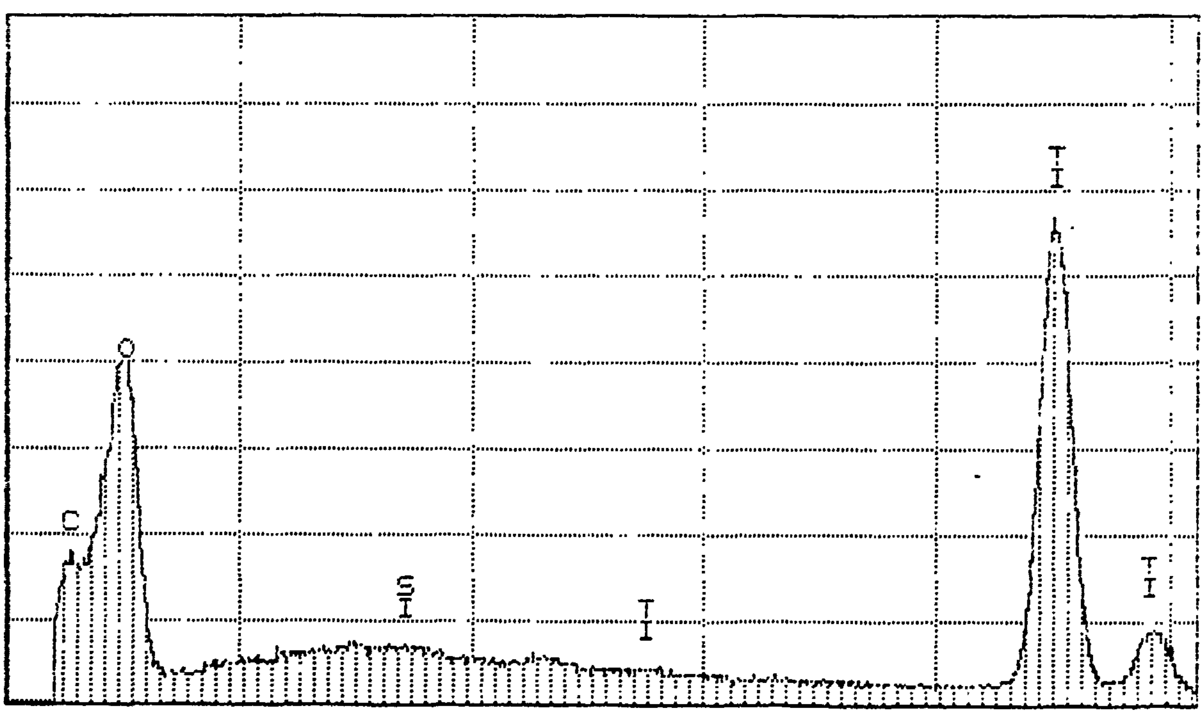

0.000 VFS = 4096 5.120
123 TIBC-2 INSIDE WEAR SPOT (UTW) 10KV

Series II Southwest Research Institute THU 03-OCT-91 14:23

Cursor: 0.000KeV = 0

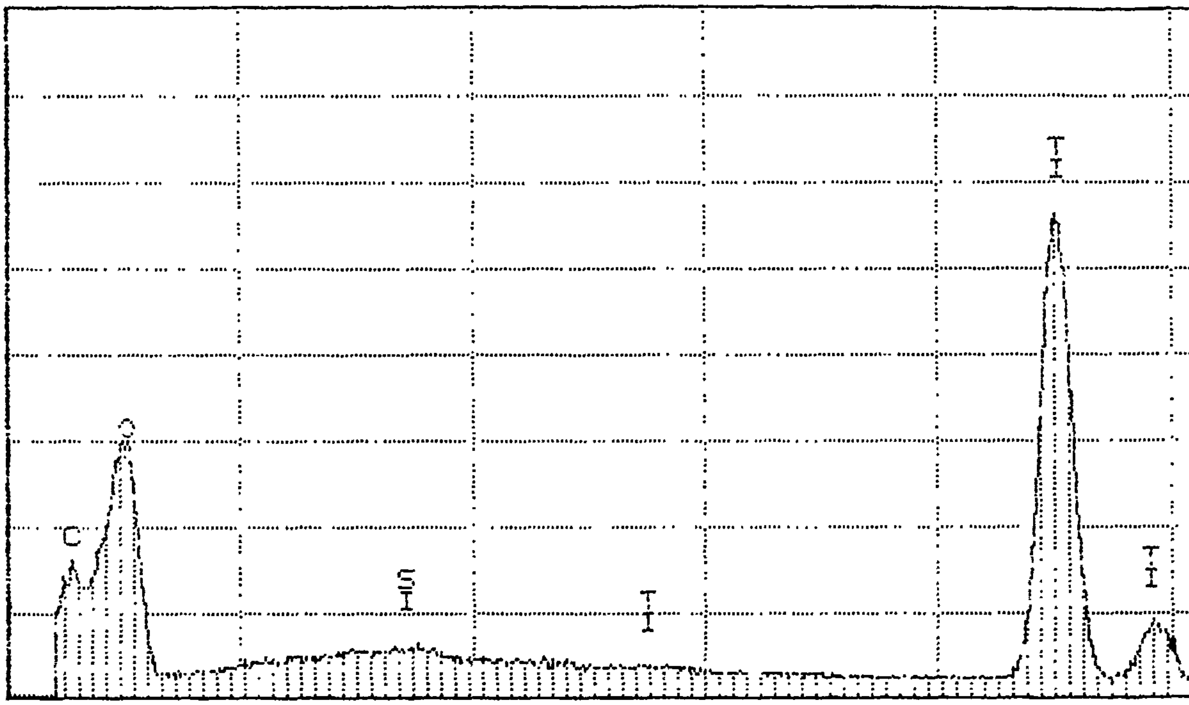

0.000 VFS = 4096 5.120

131 TIBC-2 OUTSIDE WEAR SPOT (UTW) 10KV

Series II Southwest Research Institute THU 03-OCT-91 15:00
Cursor: 0.000keV = 0

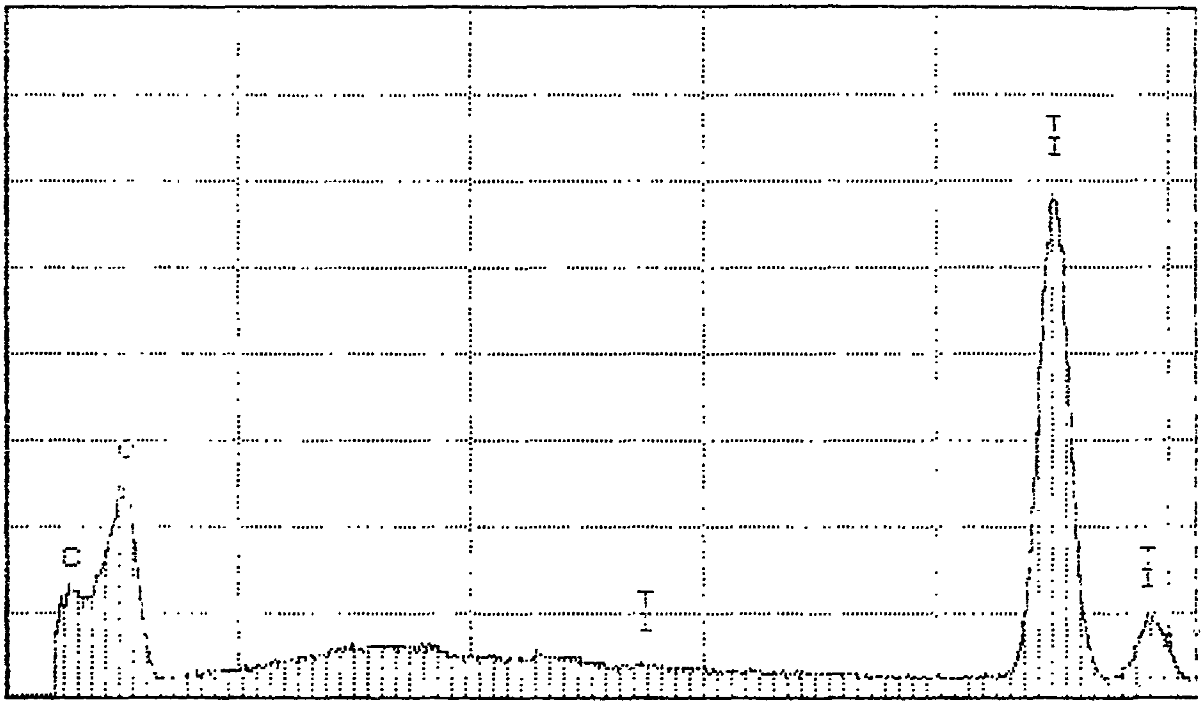

0.000 VFS = 4096 5.120
156 TIBC2/8 DEBRIS INSIDE WEAR TR. (UTW) 10KV

Series II Southwest Research Institute THU 03-OCT-91 15:05
Cursor: 0.000keV = 0

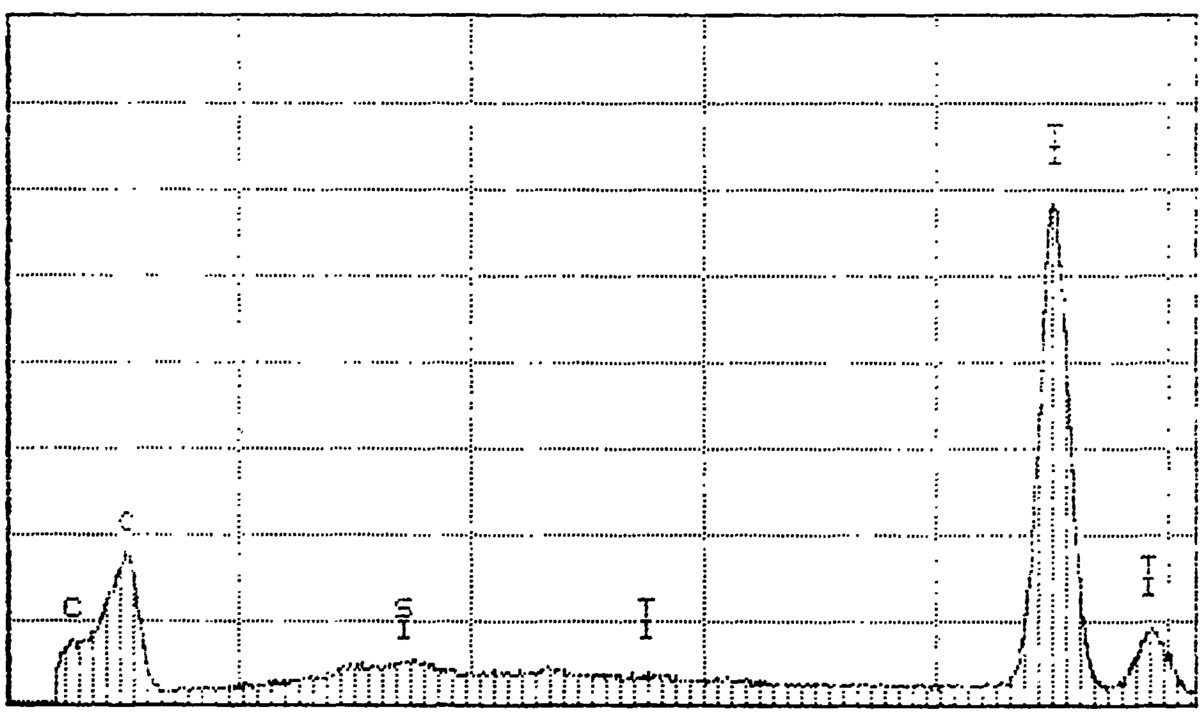

0.000 VFS = 4096 5.120
158 TIBC2/8 DEBRIS ADJACENT WEAR TR. (UTW) 10KV

Series II Southwest Research Institute THU 03-OCT-91 15:10

Cursor: 0.000KeV = 0

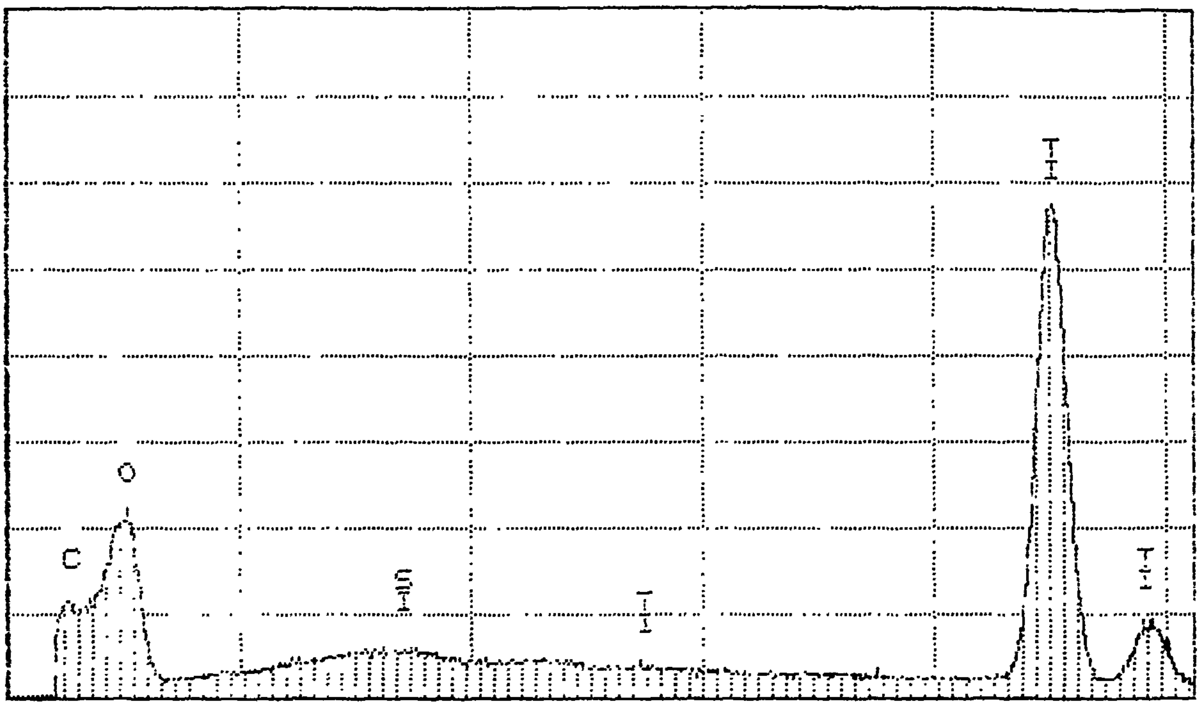

0.000 VFS = 4096 5.120

153 TIBC2/8 OUTSIDE WEAR TRACK (UTW) 10KV